

Supporting Information for: Unusual *para*-substituent effects on the intramolecular hydrogen-bond in hydrazone-based switches

Xin Su^a, Märt Lõkov^b, Agnes Kütt^b, Ivo Leito^{*b} and Ivan Aprahamian^{*a}

^a*Department of Chemistry, Dartmouth College, Hanover, New Hampshire 03755, USA.*

^b*Institute of Chemistry, University of Tartu, Ravila 14a, 50411 Tartu, Estonia.*

E-mail: ivan.aprahamian@dartmouth.edu; ivo.leito@ut.ee

Website: www.dartmouth.edu/~aprahamian/

Table of Contents

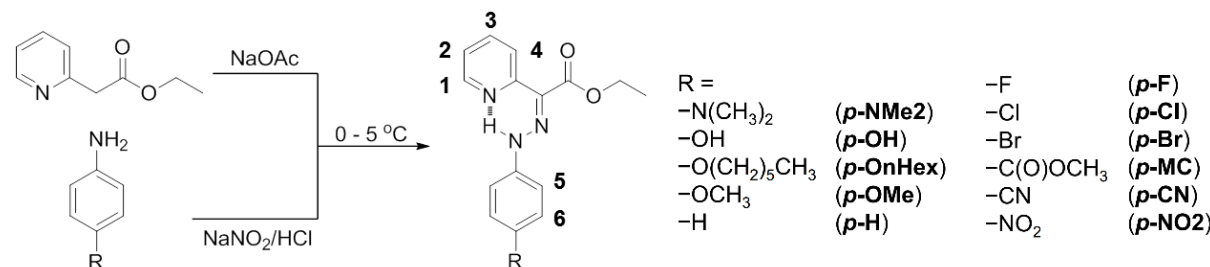
1 General	S1
2 Synthesis	S1
3 Summary of Analyzed Data	S4
4 pK_a Measurements Data	S5
5 Analysis Plots	S6
6 Single Crystal Diffraction	S9
7 Computational Methods	S13
8 NMR Spectra	S18

1 General

All reagents and starting materials were purchased from commercial sources and used as supplied unless otherwise indicated. All experiments were conducted in air unless otherwise noted. Column chromatography was performed on silica gel (SiliCycle[®], 60 Å, 230-400 mesh). Deuterated solvents were purchased from Cambridge Isotope Laboratories, Inc. and used as received. NMR spectra were recorded on a Varian Mercury 300 MHz NMR spectrometer, with working frequencies of 299.97 MHz for ¹H nuclei and 75.44 MHz for ¹³C nuclei, respectively. Chemical shifts are quoted in ppm relative to tetramethylsilane (TMS), using the residual solvent peak as the reference standard. Mass spectra were obtained either on a Shimadzu GCMS-QP2010S gas chromatograph/ EI mass spectrometer or on a Waters Quattro II ESI mass spectrometer. Melting points were measured on an Electrothermal Thermo Scientific IA9100X1 digital melting point instrument. The pK_a measurements were conducted using a previously reported methodology.^{S1,S2}

2 Synthesis

Compound **p-H** was synthesized by following a reported procedure.^{S3} All other hydrazone derivatives were synthesized in a similar manner starting from the corresponding *p*-substituted anilines and ethyl-2-pyridyl acetate.



Scheme S1: The synthesis and structures of the hydrazone derivatives with different *para*-substituents on the phenyl ring.

p-NMe₂: obtained as a red crystalline powder, yield 79%, m.p. 99.2 – 99.4 °C; ¹H NMR (300 MHz, CD₃CN) δ 14.78 (s, N–H), 8.68 (ddd, *J*= 5.0, 1.9, 1.0 Hz, H1), 8.19 (dt, *J*= 8.4, 1.0 Hz, H4), 7.87 (ddd, *J*= 8.4, 7.5, 1.9 Hz, H3), 7.47 – 7.21 (m, H2 and H5), 6.88 – 6.70 (d, *J*= 9.0 Hz, H6), 4.30 (qd, *J*= 7.1, 1.8 Hz, –CH₂–), 2.89 (s, –N(CH₃)₂), 1.37 (t, *J*= 7.1 Hz, –CH₃)

ppm; ^{13}C NMR (75 MHz, CD_3CN) δ 166.47, 153.88, 148.54, 147.55, 137.71, 134.92, 124.51, 124.36, 123.83, 122.92, 116.70, 116.37, 114.60, 61.27, 41.14, 14.64 ppm. MS (ESI): m/z found [M–H $^+$] for $\text{C}_{17}\text{H}_{21}\text{N}_4\text{O}_2^+$ 313.2 (calcd. 313.2).

p-OH: obtained as a yellow powder, yield 82%, m.p. 178.9 – 179.3 °C; ^1H NMR (300 MHz, CD_3CN) δ 14.64 (s, N–H), 8.70 (d, J = 5.0 Hz, H1), 8.16 (d, J = 8.4 Hz, H4), 7.97 – 7.83 (m, H3), 7.34 (dd, J = 6.5, 5.1 Hz, H2), 7.24 (d, J = 8.9 Hz, H5), 6.83 (d, J = 8.9 Hz, H6), 6.74 (s, –OH), 4.31 (q, J = 7.1 Hz, –CH $_2$ –), 1.37 (t, J = 7.1 Hz, –CH $_3$) ppm; ^{13}C NMR (75 MHz, CD_3CN) δ 166.38, 153.84, 153.67, 147.71, 137.84, 137.47, 137.18, 125.29, 124.71, 123.23, 116.88, 116.83, 116.51, 61.41, 14.62 ppm. MS (ESI): m/z found [M–H $^+$] for $\text{C}_{15}\text{H}_{16}\text{N}_3\text{O}_3^+$ 286.1 (calcd. 286.1).

p-OnHex: obtained as bright yellow flakes, yield 89%, m.p. 74.0 – 74.4 °C; ^1H NMR (300 MHz, CD_3CN) δ 14.67 (s, N–H), 8.75 – 8.66 (m, H1), 8.16 (d, J = 8.4 Hz, H4), 7.87 (ddd, J = 24.0, 12.6, 8.7 Hz, H3), 7.36 – 7.27 (m, H2 and H5), 6.90 (dd, J = 10.3, 5.6 Hz, H6), 4.31 (q, J = 7.1 Hz, –OCH $_2\text{CH}_3$), 3.94 (dd, J = 9.0, 4.1 Hz, –OCH $_2\text{CH}_2$ –), 1.83 – 1.64 (m, –OCH $_2\text{CH}_2$ –), 1.55 – 1.20 (m, –CH $_2\text{CH}_2\text{CH}_2\text{CH}_2\text{CH}_3$ and –OCH $_2\text{CH}_3$), 0.91 (dd, J = 9.6, 4.3 Hz, –CH $_2\text{CH}_2\text{CH}_3$) ppm; ^{13}C NMR (75 MHz, CD_3CN) δ 166.34, 156.16, 153.55, 147.69, 137.93, 137.83, 125.53, 124.71, 123.26, 116.64, 116.36, 116.21, 69.06, 61.43, 32.23, 29.92, 26.34, 23.24, 14.59, 14.25 ppm. MS (EI): m/z found M $^+$ for $\text{C}_{21}\text{H}_{27}\text{N}_3\text{O}_3^+$ 369 (calcd. 369).

p-OMe: obtained as a dark yellow powder, yield 69%, m.p. 71.9 – 72.3 °C; ^1H NMR (300 MHz, CD_3CN) δ 14.66 (s, N–H), 8.70 (ddd, J = 5.0, 1.8, 0.9 Hz, H1), 8.15 (dt, J = 8.3, 0.9 Hz, H4), 7.88 (ddd, J = 8.4, 7.6, 1.9 Hz, H3), 7.39 – 7.27 (m, H2 and H5), 6.94 (d, J = Hz, H6), 4.31 (q, J = 7.1 Hz, –CH $_2$ –), 3.77 (s, –OCH $_3$), 1.37 (t, J = 7.1 Hz, –CH $_2\text{CH}_3$) ppm; ^{13}C NMR (75 MHz, CD_3CN) δ 166.35, 156.72, 153.59, 147.74, 138.11, 137.88, 125.65, 124.76, 123.32, 116.67, 116.33, 115.61, 115.55, 61.46, 56.07, 14.62 ppm. MS (EI): m/z found M $^+$ for $\text{C}_{16}\text{H}_{17}\text{N}_4\text{O}_2^+$ 299 (calcd. 299).

p-F: obtained as a bright yellow powder, yield 75%, m.p. 61.7 – 62.0 °C; ^1H NMR (300 MHz, CD_3CN) δ 14.60 (s, N–H), 8.71 (ddd, J = 5.0, 1.8, 1.0 Hz, H1), 8.12 (dt, J = 8.3, 1.0 Hz, H4), 7.90 (ddd, J = 8.4, 7.6, 1.9 Hz, H3), 7.46 – 7.33 (m, H2 and H5), 7.17 – 7.02 (m, H6), 4.33

(qd, $J = 7.1, 1.9$ Hz, $-\text{CH}_2-$), 1.38 (t, $J = 7.2$ Hz, $-\text{CH}_3$) ppm; ^{13}C NMR (75 MHz, CD_3CN) δ 166.17, 161.11, 157.95, 153.20, 147.89, 140.95, 138.01, 129.91, 124.98, 123.69, 116.94, 116.75, 116.65, 61.65, 14.55 ppm. MS (EI): m/z found M^+ for $\text{C}_{15}\text{H}_{14}\text{FN}_3\text{O}_2^+$ 287 (calcd. 287).

p-Cl: obtained as a bright yellow powder, yield 81%, m.p. $85.9 - 86.3$ °C; ^1H NMR (300 MHz, CD_3CN) δ 14.58 (s, N–H), 8.72 (ddd, $J = 5.0, 1.9, 1.0$ Hz, H1), 8.10 (dt, $J = 8.3, 1.0$ Hz, H4), 7.98 – 7.84 (m, H3), 7.49 – 7.17 (m, H2, H5 and H6), 4.32 (qd, $J = 7.2, 4.2$ Hz, $-\text{CH}_2-$), 1.36 (t, $J = 7.2$ Hz $-\text{CH}_3$) ppm; ^{13}C NMR (75 MHz, CD_3CN) δ 166.07, 152.99, 147.98, 143.35, 138.75, 138.08, 130.14, 127.57, 125.14, 124.19, 123.90, 117.66, 116.73, 61.77, 14.52 ppm. MS (EI): m/z found M^+ for $\text{C}_{15}\text{H}_{14}\text{ClN}_3\text{O}_2^+$ 303 (calcd. 303) and $\text{C}_{15}\text{H}_{14}\text{ClN}_3\text{O}_2^+$ 305 (calcd. 305).

p-Br: obtained as a bright yellow powder, yield 83%, m.p. $91.5 - 92.0$ °C; ^1H NMR (300 MHz, CD_3CN) δ 14.57 (s, 1H), 8.78 – 8.66 (m, H1), 8.10 (dt, $J = 8.3, 1.0$ Hz, H4), 8.01 – 7.85 (m, H3), 7.54 – 7.45 (m, H6), 7.39 (ddd, $J = 7.5, 5.0, 1.1$ Hz, H2), 7.33 – 7.25 (m, H5), 4.33 (qd, $J = 7.1, 2.8$ Hz, $-\text{CH}_2-$), 1.37 (t, $J = 7.2$ Hz CH_3) ppm; ^{13}C NMR (75 MHz, CD_3CN) δ 166.07, 153.02, 149.61, 148.03, 143.83, 138.12, 133.11, 128.05, 125.20, 123.95, 117.15, 116.83, 115.04, 61.80, 14.56 ppm. MS (EI): m/z found M^+ for $\text{C}_{15}\text{H}_{14}\text{BrN}_3\text{O}_2^+$ 347 (calcd. 347) and $\text{C}_{15}\text{H}_{14}\text{BrN}_3\text{O}_2^+$ 349 (calcd. 350).

p-MC: obtained as a bright yellow powder, yield 80%, m.p. $92.7 - 93.1$ °C; ^1H NMR (300 MHz, CD_3CN) δ 14.64 (s, N–H), 8.79 – 8.70 (m, H1), 8.07 (dt, $J = 8.3, 1.0$ Hz, 4H), 8.02 – 7.87 (m, H3 and H5), 7.47 – 7.36 (m, H2 and H6), 4.35 (qd, $J = 7.1, 1.9$ Hz, $-\text{CH}_2-$), 3.84 (s, $-\text{OCH}_3$), 1.38 (t, $J = 7.2$ Hz, $-\text{CH}_2\text{CH}_3$) ppm; ^{13}C NMR (75 MHz, CD_3CN) δ 167.31, 165.95, 152.69, 148.32, 148.20, 138.25, 131.98, 129.71, 125.44, 124.60, 124.29, 116.11, 114.79, 62.00, 52.37, 14.53 ppm. MS (EI): m/z found M^+ for $\text{C}_{17}\text{H}_{17}\text{N}_3\text{O}_4^+$ 327 (calcd. 327).

p-CN: obtained as a bright yellow powder, yield 80%, m.p. $95.7 - 95.9$ °C; ^1H NMR (300 MHz, CD_3CN) δ 14.65 (s, N–H), 8.84 – 8.65 (m, H1), 8.06 (d, $J = 8.3$ Hz, H4), 7.99 – 7.88 (m, H3), 7.65 (d, $J = 7.7$ Hz, H5), 7.49 – 7.28 (m, H2 and H6), 4.35 (q, $J = 7.1$ Hz, $-\text{CH}_2-$), 1.38 (t, $J = 7.1$ Hz, $-\text{CH}_3$) ppm; ^{13}C NMR (75 MHz, CD_3CN) δ 165.80, 152.40, 150.76, 149.56, 148.22, 138.30, 135.13, 134.65, 129.90, 125.51, 124.48, 120.18, 115.46, 105.07, 62.09, 14.46 ppm. MS (EI): m/z found M^+ for $\text{C}_{16}\text{H}_{14}\text{N}_4\text{O}_2^+$ 294 (calcd. 294).

p-NO₂: obtained as a bright yellow powder, yield 77%, m.p. 124.2 – 124.5 °C; ¹H NMR (300 MHz, CD₃CN) δ 14.77 (s, N–H), 8.75 (ddd, *J*= 4.9, 1.8, 1.0 Hz, H1), 8.25 – 8.13 (m, H6), 8.05 (dt, *J*= 8.2, 1.0 Hz, H4), 7.99 – 7.90 (m, H3), 7.49 – 7.38 (m, H2 and H5), 4.37 (dq, *J*= 14.2, 7.0 Hz, –CH₂–), 1.39 (t, *J*= 7.1 Hz, –CH₃) ppm; ¹³C NMR (75 MHz, CD₃CN) δ 201.96, 165.68, 152.17, 149.87, 148.28, 142.90, 138.36, 131.51, 126.55, 125.61, 124.66, 114.77, 114.42, 110.52, 62.19, 14.42 ppm. MS (EI): *m/z* found M⁺ for C₁₅H₁₄N₄O₄⁺ 314 (calcd. 314).

3 Summary of Analyzed Data

Table S1: A summary of Hammett constants, chemical shifts (CD₃CN), N···N distances and pK_a values.

	σ_p	$\delta_{N-H,Z}/\text{ppm}$	$\delta_{N-H,E}/\text{ppm}$	δ_{H5}/ppm	$d(N \cdots N)/\text{\AA}$	pK _a
p-NMe₂	-0.83	11.85	14.78	8.68	2.6349(14)	13.39
p-OH	-0.37	11.67	14.64	8.69	-	12.92
p-OnHex	-0.34	11.67	14.67	8.69	2.6312(37)	12.86
p-OMe	-0.27	11.66	14.66	8.70	-	12.82
p-H	0	11.48	14.55	8.72	2.6580(23)	12.26
p-F	0.06	11.46	14.60	8.71	-	12.26
p-Cl	0.23	11.36	14.58	8.72	2.6198(32)	12.08
p-Br	0.23	11.34	14.57	8.72	2.6280(27)	12.08
p-MC	0.45	11.290	14.643	8.744	-	11.6
p-CN	0.66	11.15	14.65	8.74	-	11.4
p-NO₂	0.78	11.16	14.77	8.75	2.6027(16)	10.2

4 pK_a Measurements Data

Table S2: Results of the experimental pK_a measurements.

Base (B)	Reference base (RB)	pK_a RB ^a	ΔpK_a $pK_a(RB) - pK_a(B)$	pK_a (B)	$pK_a(B)$ Assigned
p-NMe₂	2-Me-Pyridine	13.32	-0.09	13.41	13.39
	2,6-Me ₂ -Pyridine	14.13	0.76	13.37	
p-OH	Pyridine	12.53	-0.36	12.89	12.92
	2-Me-Pyridine	13.32	0.38	12.94	
p-OnHex	Pyridine	12.53	-0.28	12.81	12.86
	2-Me-Pyridine	13.32	0.38	12.94	
p-OMe	2-Me-Pyridine	13.32	0.47	12.85	12.82
	Pyridine	12.53	-0.26	12.79	
p-H	4-MeO-Aniline	11.86	-0.40	12.26	12.26
	2-Me-Aniline	10.50	-1.71	12.21	
	Pyridine	12.53	0.22	12.31	
p-F	4-MeO-Aniline	11.86	-0.39	12.25	12.26
	Pyridine	12.53	0.39	12.26	
p-Cl	Pyridine	12.53	0.44	12.09	12.08
	4-MeO-Aniline	11.86	-0.21	12.07	
p-Br	4-MeO-Aniline	11.86	-0.16	12.02	12.08
	Pyridine	12.53	0.39	12.14	
p-MC	Aniline	10.62	-0.89	11.51	11.6
	4-MeO-Aniline	11.86	0.16	11.70	
	N,N-Me ₂ -Aniline	11.43	-0.14	11.57	
p-CN	2-Me-Aniline	10.50	-0.57	11.07	11.4
	4-MeO-Aniline	11.86	0.42	11.44	
	N,N-Me ₂ -Aniline	11.43	-0.02	11.45	
p-NO₂	N,N-Me ₂ -Aniline	11.43	0.88	10.55	10.2
	2-Me-Aniline	10.50	0.71	9.79	

^a pK_a values of reference bases were taken from Refs. S1 and S2.

5 Analysis Plots

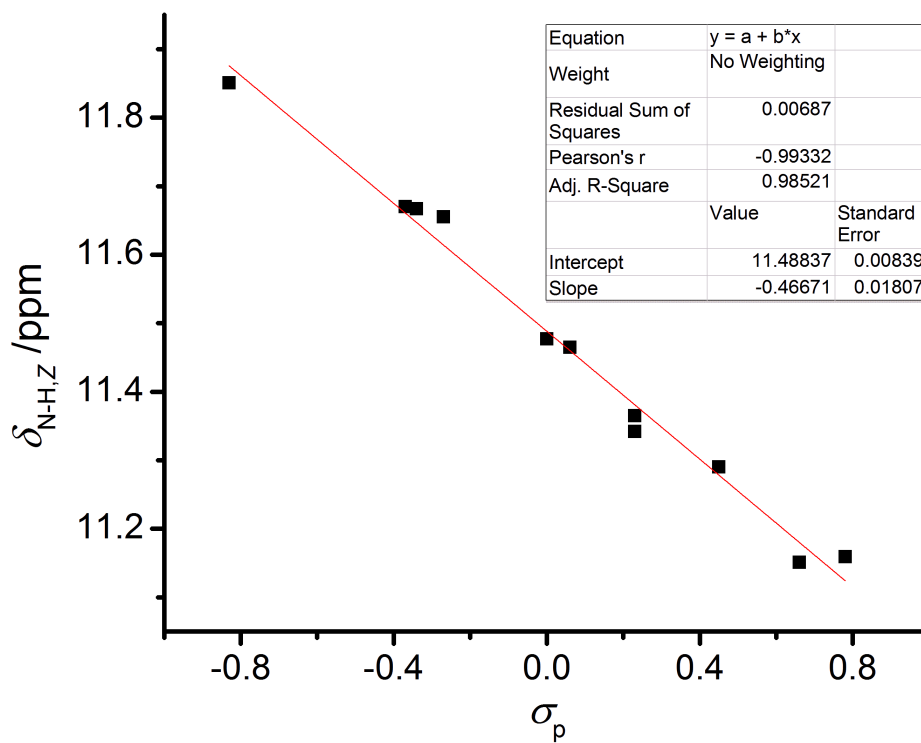


Figure S1: The plot of $\delta_{N-H,Z}$ of the different derivatives (Z configuration) vs. the corresponding σ_p values, and the linear regression fitting results.

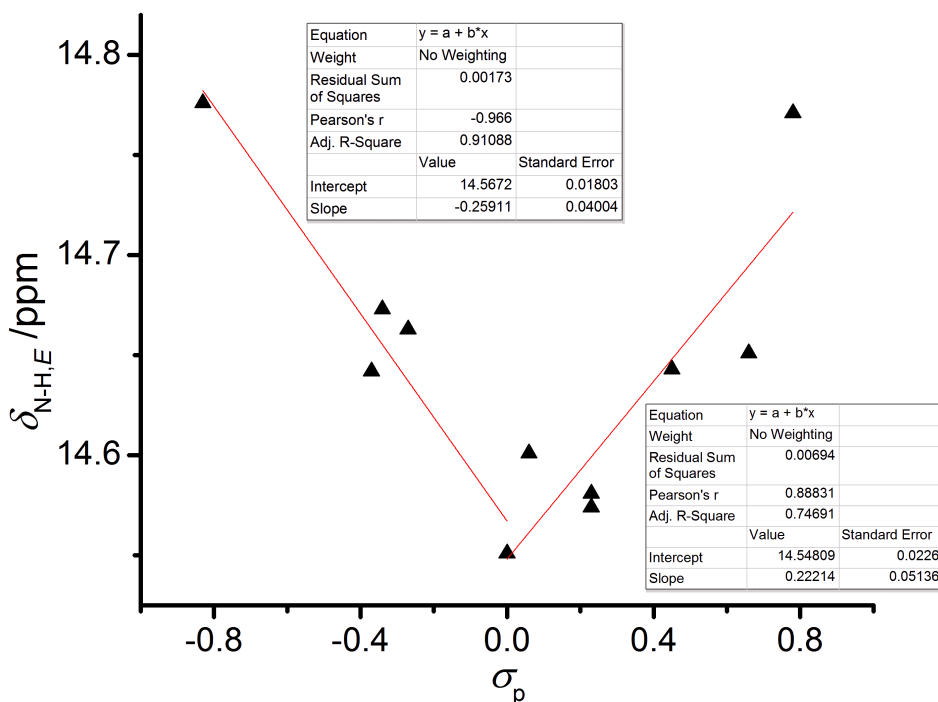


Figure S2: The plot of $\delta_{N-H,E}$ of the different derivatives (E configuration) vs. the corresponding σ_p values, and the linear regression fitting results.

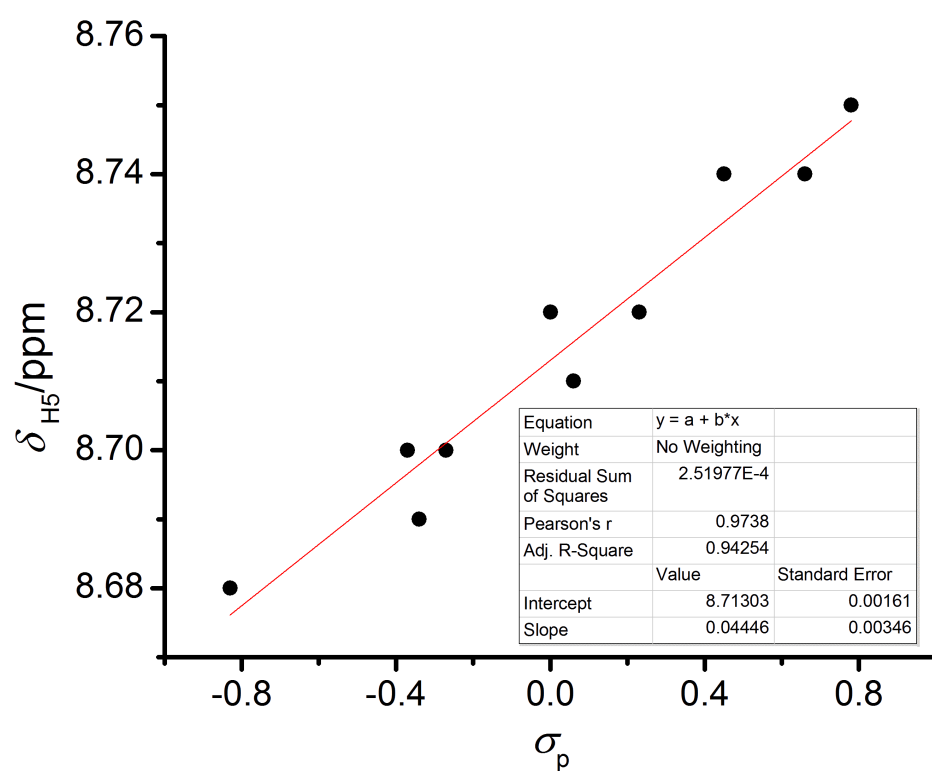


Figure S3: The plot of δ_{H5} of the different derivatives *vs.* the corresponding σ_p values, and the linear regression fitting results.

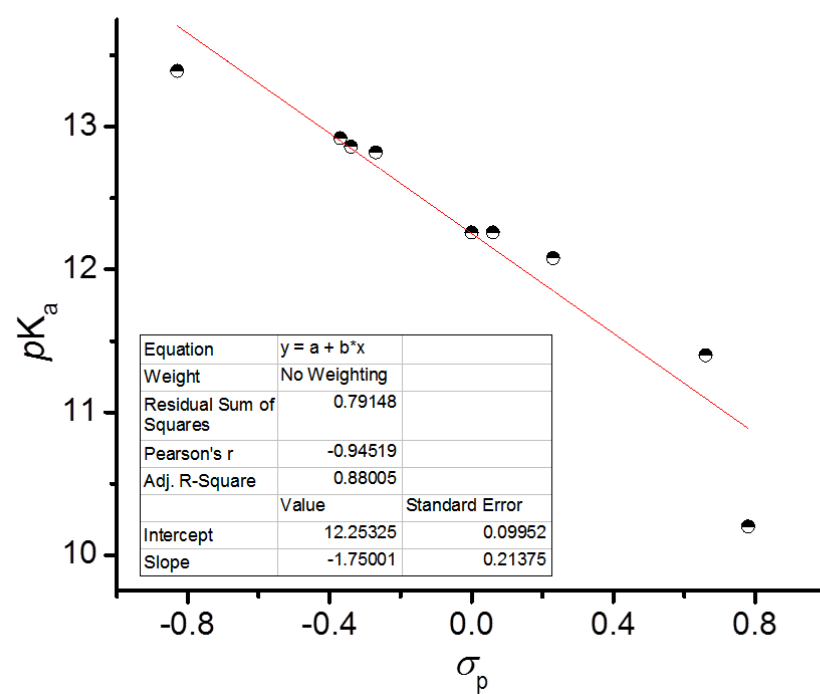


Figure S4: The plot of the pK_a s of the different derivatives *vs.* the corresponding σ_p values, and the linear regression fitting results.

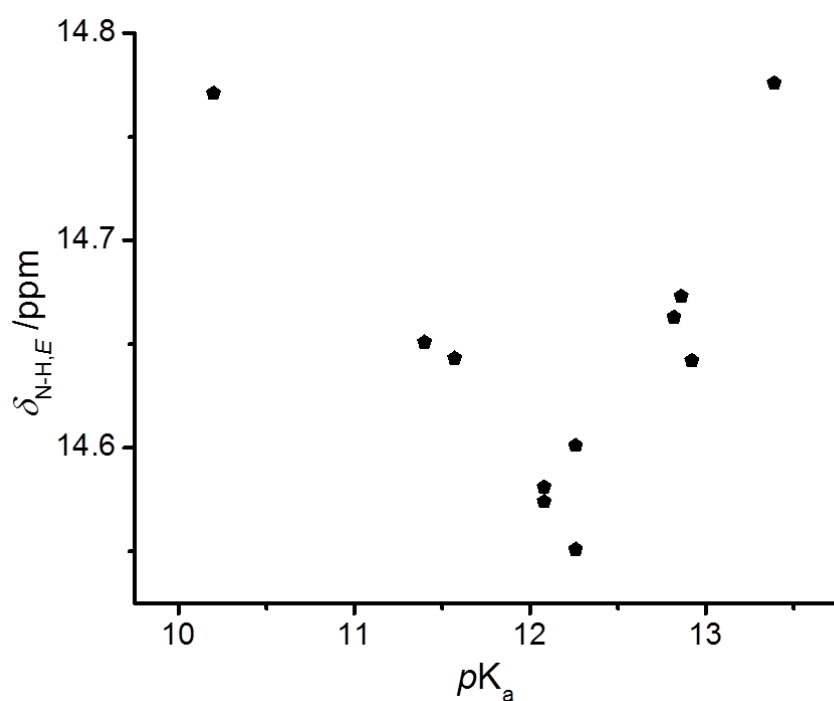


Figure S5: The plot of $\delta_{N-H,E}$ of the different derivatives (*E* configuration) vs. the corresponding pK_a values.

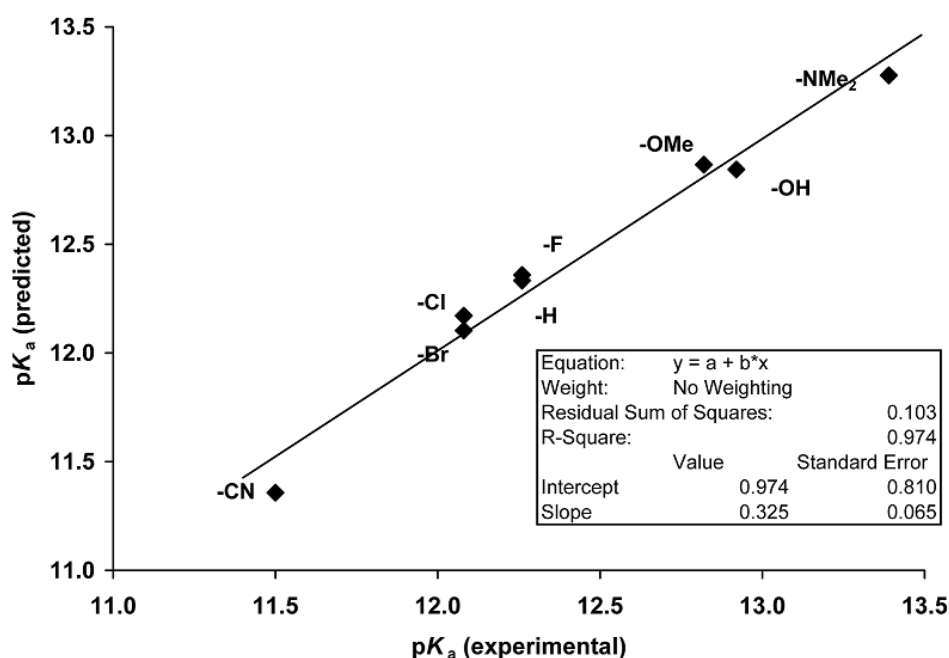


Figure S6: The plot of the predicted pK_a values of the different derivatives vs. the corresponding experimental pK_a values, and the linear regression fitting results.

6 Single Crystal Diffraction

Data were collected using a Bruker CCD (charge coupled device) based diffractometer equipped with an Oxford Cryostream low-temperature apparatus operating at 173 K. Data were measured using ω and ϕ scans of 0.5° per frame for 30 s. The total number of images was based on results from the program COSMO^{S4} where redundancy was expected to be 4.0 and completeness of 100% out to 0.83 Å. Cell parameters were retrieved using APEX II software^{S5} and refined using SAINT on all observed reflections. Data reduction was performed using the SAINT software^{S6} which corrects for L_p . Scaling and absorption corrections were applied using SADABS^{S7} multi-scan technique, supplied by George Sheldrick. The structures are solved by the direct method using the SHELXS-97 program and refined by least squares method on F^2 , SHELXL-97, which are incorporated in SHELXTL-PC V 6.10.^{S8} All non-hydrogen atoms are refined anisotropically. All hydrogens were calculated by geometrical methods and refined as a riding model.

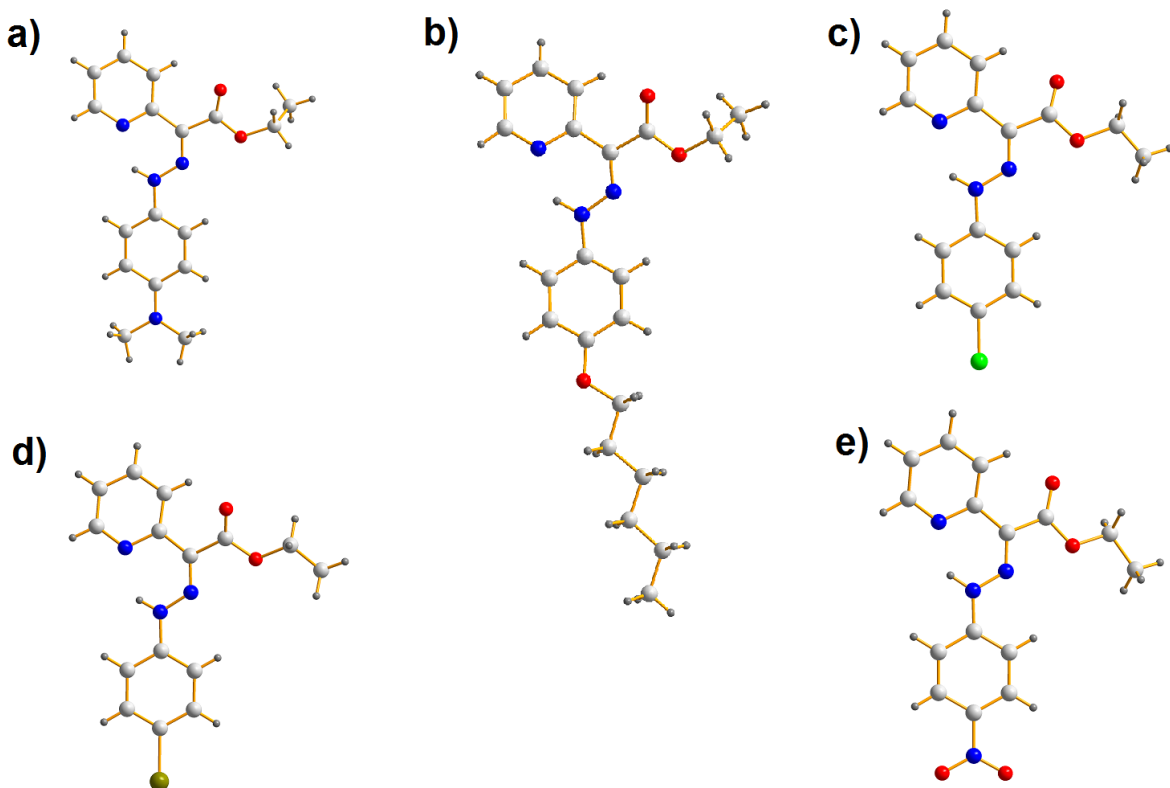


Figure S7: Ball-stick drawings of the crystal structures of *p*-NMe₂(a), *p*-OnHex(b), *p*-Cl(c), *p*-Br(d) and *p*-NO₂(e).

Table S3: Crystal data and parameters for **p-NMe₂**, **p-OnHex**, **p-Cl**, **p-Br** and **p-NO₂**.

	p-NMe₂	p-OnHex
CCDC	885513	885514
Empirical formula	C ₁₇ H ₂₀ N ₄ O ₂	C ₂₁ H ₂₇ N ₃ O ₃
Formula weight	312.37	369.46
Temperature	173(2) K	173(2) K
Wavelength	0.71073 Å	1.54178 Å
Crystal system	Monoclinic	Monoclinic
Space group	P2 ₁ /c	P2 ₁ /c
Unit cell dimensions	a = 18.9390(13) Å α = 90° b = 7.5769(5) Å β = 93.5940(10)° c = 11.1814(8) Å γ = 90°	a = 21.5273(7) Å α = 90° b = 14.3929(5) Å β = 96.137(3)° c = 6.4359(2) Å γ = 90°
Volume	1333.2(2) Å ³	1982.67(11) Å ³
Z	4	4
Density (calcd.)	1.296 Mg·m ⁻³	1.238 Mg·m ⁻³
Absorption coefficient	0.088 mm ⁻¹	0.673 mm ⁻¹
F ₀₀₀	664	792
Crystal size	0.37 × 0.24 × 0.17 mm ³	0.20 × 0.14 × 0.08 mm ³
θ range for data collection	2.15 to 25.32°	2.06 to 68.23°
Index ranges	-22 ≤ h ≤ 22 -9 ≤ k ≤ 9 -13 ≤ l ≤ 13	-25 ≤ h ≤ 25 -14 ≤ k ≤ 16 -7 ≤ l ≤ 7
Reflections collected	25125	14479
Independent reflections	2925 [R _{int} = 0.0263]	3505 [R _{int} = 0.0981]
Completeness to θ = 25.36°	99.9%	96.7%
Absorption correction	Semi-empirical from equivalents	Semi-empirical from equivalents
Max. and min. transmission	0.9849 and 0.9685	0.9500 and 0.8743
Refinement method	Full-matrix least-squares on F ²	Full-matrix least-squares on F ²
Data / restraints / parameters	2925 / 0 / 211	3505 / 0 / 352
Goodness-of-fit on F ²	1.039	1.014
Final R indices [I > 2σ(I)]	R ₁ = 0.0324, ωR ₂ = 0.0854	R ₁ = 0.0594, ωR ₂ = 0.1154
R indices (all data)	R ₁ = 0.0367, ωR ₂ = 0.0900	R ₁ = 0.1220, ωR ₂ = 0.1399
Largest diff. peak and hole	0.143 and -0.202 e·Å ⁻³	0.437 and -0.238 e·Å ⁻³

(Continued)

	<i>p</i> -Cl	<i>p</i> -Br
CCDC	885515	885516
Empirical formula	C ₁₅ H ₁₄ ClN ₃ O ₂	C ₁₅ H ₁₄ BrN ₃ O ₂
Formula weight	303.74	348.20
Temperature	173(2) K	173(2) K
Wavelength	0.71073 Å	0.71073 Å
Crystal system	Orthorhombic	Orthorhombic
Space group	P2 ₁ 2 ₁ 2 ₁	P2 ₁ 2 ₁ 2 ₁
Unit cell dimensions	a = 4.9468(4) Å α = 90° b = 9.7236(7) Å β = 90° c = 29.425(2) Å γ = 90°	a = 7.2194(2) Å α = 90° b = 10.0881(3) Å β = 90° c = 20.1172(6) Å γ = 90°
Volume	1415.39(19) Å ³	1465.14(7) Å ³
Z	4	4
Density (calcd.)	1.425 Mg·m ⁻³	1.579 Mg·m ⁻³
Absorption coefficient	0.278 mm ⁻¹	2.813 mm ⁻¹
F ₀₀₀	632	704
Crystal size	0.29 × 0.22 × 0.08 mm ³	0.29 × 0.19 × 0.10 mm ³
θ range for data collection	2.21 to 25.38°	2.02 to 25.34°
Index ranges	-5 ≤ h ≤ 5 -11 ≤ k ≤ 11 -35 ≤ l ≤ 35	-8 ≤ h ≤ 5 -10 ≤ k ≤ 12 -24 ≤ l ≤ 19
Reflections collected	11499	7614
Independent reflections	2590 [R _{int} = 0.0307]	2644 [R _{int} = 0.0269]
Completeness to θ = 25.36°	99.9%	100.0%
Absorption correction	Semi-empirical from equivalents	Semi-empirical from equivalents
Max. and min. transmission	0.9781 and 0.9233	0.7623 and 0.4948
Refinement method	Full-matrix least-squares on F ²	Full-matrix least-squares on F ²
Flack parameters	-0.02(10)	0.000(9)
Data / restraints / parameters	2590 / 0 / 191	2644 / 0 / 191
Goodness-of-fit on F ²	1.049	1.001
Final R indices [I > 2σ(I)]	R ₁ = 0.0441, ωR ₂ = 0.1058	R ₁ = 0.0247, ωR ₂ = 0.0538
R indices (all data)	R ₁ = 0.0522, ωR ₂ = 0.1124	R ₁ = 0.0310, ωR ₂ = 0.0556
Largest diff. peak and hole	0.674 and -0.302 e·Å ⁻³	0.200 and -0.310 e·Å ⁻³

(Continued)

	<i>p</i> -NO ₂
CCDC	885517
Empirical formula	C ₁₅ H ₁₄ N ₄ O ₂
Formula weight	314.30
Temperature	173(2) K
Wavelength	0.71073 Å
Crystal system	Orthorhombic
Space group	Pbca
Unit cell dimensions	$a = 6.6841(5)$ Å $\alpha = 90^\circ$ $b = 19.9101(15)$ Å $\beta = 90^\circ$ $c = 22.7748(17)$ Å $\gamma = 90^\circ$ $3030.9(4)$ Å ³
Volume	3030.9(4) Å ³
Z	8
Density (calcd.)	1.378 Mg·m ⁻³
Absorption coefficient	0.103 mm ⁻¹
<i>F</i> ₀₀₀	1312
Crystal size	$0.46 \times 0.10 \times 0.08$ mm ³
θ range for data collection	1.79 to 26.46°
Index ranges	$-8 \leq h \leq 8$ $-23 \leq k \leq 24$ $-28 \leq l \leq 28$
Reflections collected	24984
Independent reflections	3134 [$R_{\text{int}} = 0.0449$]
Completeness to $\theta = 25.36^\circ$	99.9%
Absorption correction	Semi-empirical from equivalents
Max. and min. transmission	0.9920 and 0.9542
Refinement method	Full-matrix least-squares on <i>F</i> ²
Data / restraints / parameters	3134 / 0 / 264
Goodness-of-fit on <i>F</i> ²	1.011
Final <i>R</i> indices [$I > 2\sigma(I)$]	$R_1 = 0.0360$, $\omega R_2 = 0.0836$
<i>R</i> indices (all data)	$R_1 = 0.0573$, $\omega R_2 = 0.0954$
Largest diff. peak and hole	0.162 and -0.187 e·Å ⁻³

7 Computational Methods

Calculations were performed using density functional theory (DFT) with the B3LYP functional^{S9} as implemented in Gaussian 09.^{S10} Geometry optimizations and frequency analysis were performed using the 6-311+G(d) basis set. NBO calculations were done using the B3LYP optimized structures.

Table S4: A summary of the NBO calculated charge distributions on the N–H and the pyridyl nitrogens in *p*-NMe₂, *p*-H and *p*-NO₂.

	N–H Nitrogen	Pyridyl Nitrogen
<i>p</i> -NMe ₂	-0.331	-0.536
<i>p</i> -H	-0.357	-0.526
<i>p</i> -NO ₂	-0.345	-0.530

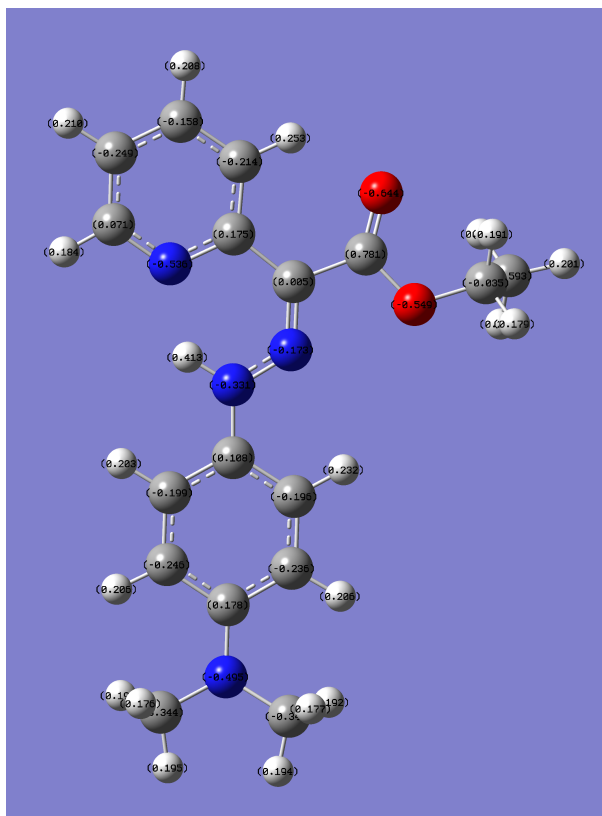


Figure S8: Ball-and-stick drawing of the B3LYP/6-311+G(d) optimized structure of *p*-NMe₂. The NBO calculated charge distribution is shown as well.

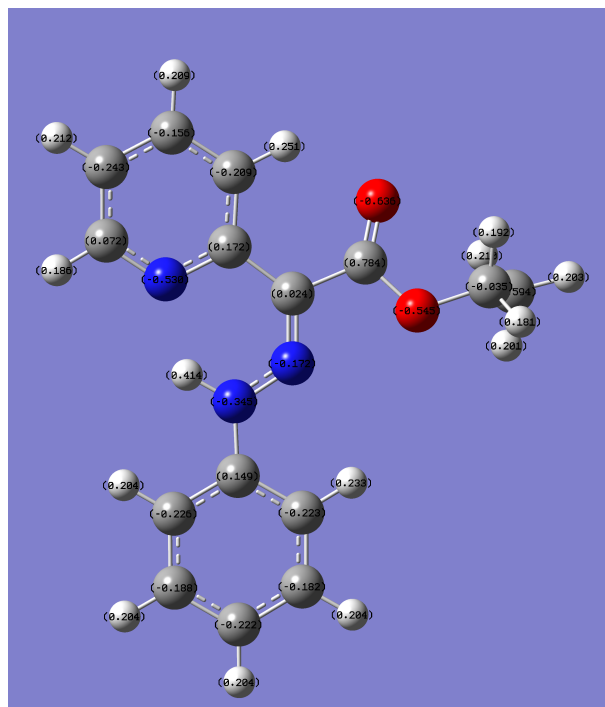


Figure S9: Ball-and-stick drawing of the B3LYP/6-311+G(d) optimized structure of *p*-H. The NBO calculated charge distribution is shown as well.

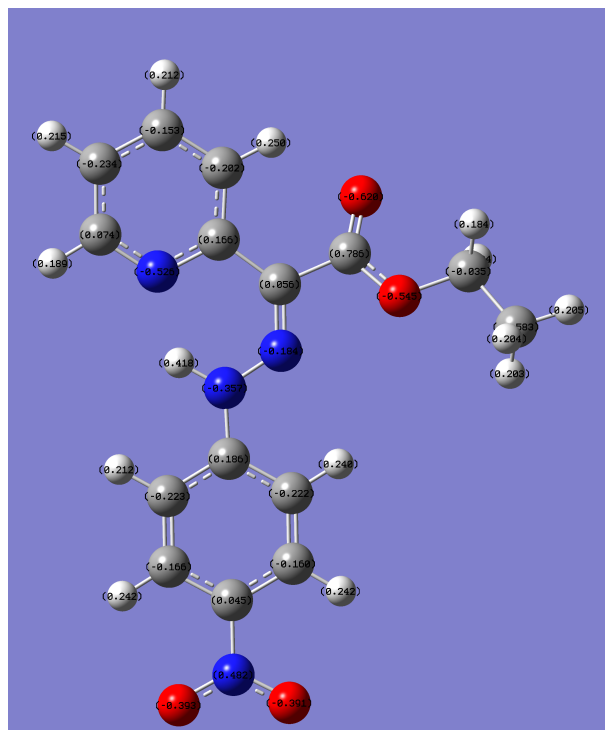


Figure S10: Ball-and-stick drawing of the B3LYP/6-311+G(d) optimized structure of *p*-NO₂. The NBO calculated charge distribution is shown as well.

Table S5: Cartesian coordinates for the B3LYP/6-311+G(d) optimized structure of *p*-NMe₂.

O	13.354285	4.5082	5.199623
O	11.130906	4.182351	5.196485
N	14.06781	2.915084	8.606348
H	13.349289	2.60197	9.26945
N	13.666881	3.405644	7.469328
N	11.518283	2.611802	9.185815
N	19.52514	2.404847	9.926753
C	15.436945	2.810382	8.907531
C	16.434185	3.247536	8.032106
H	16.149887	3.687117	7.084163
C	17.772711	3.127735	8.37557
H	18.509827	3.485857	7.669073
C	18.178346	2.558678	9.60386
C	17.155065	2.140238	10.480456
H	17.395061	1.714856	11.445742
C	15.81565	2.259712	10.133772
H	15.05635	1.923836	10.83457
C	20.522034	3.107086	9.135952
H	20.488556	2.791621	8.090122
H	21.514103	2.863075	9.513915
H	20.401096	4.200409	9.167523
C	19.883302	2.063993	11.292756
H	19.558537	2.820826	12.02298
H	20.965674	1.964422	11.364391
H	19.450518	1.103461	11.58405
C	12.397323	3.535192	7.139237
C	12.202084	4.093933	5.769328
C	13.267436	5.027642	3.854604
H	14.122715	5.700606	3.777845
H	12.348312	5.60536	3.751031
C	13.343667	3.919067	2.817707
H	14.251169	3.324275	2.947714
H	13.361823	4.351751	1.812486
H	12.478302	3.257487	2.885097
C	11.236351	3.178773	7.98599
C	9.893831	3.416182	7.61842
H	9.674764	3.861452	6.661317
C	8.875894	3.061438	8.489721
H	7.842926	3.242416	8.209325
C	9.183611	2.475029	9.717125
H	8.413143	2.183313	10.421866
C	10.524672	2.27549	10.011603
H	10.825537	1.824858	10.954247

Table S6: Cartesian coordinates for the B3LYP/6-311+G(d) optimized structure of *p*-H.

O	4.286749	9.236076	5.553032
O	3.020645	9.429371	7.400530
N	4.218824	11.747371	5.097162
N	4.289886	12.970012	4.639244
H	3.659487	13.669066	5.046512
N	2.351764	13.536336	6.339138
C	3.521307	9.934575	6.413635
C	3.367540	11.371162	6.021811
C	2.340632	12.222295	6.670004
C	1.366127	11.725404	7.560085
H	1.367746	10.680969	7.827964
C	0.427547	12.594772	8.095381
H	-0.324158	12.217241	8.781277
C	0.457366	13.945100	7.751158
H	-0.258241	14.653681	8.152500
C	1.442706	14.359717	6.865722
H	1.512073	15.400111	6.558417
C	4.548015	7.852290	5.882975
H	4.743091	7.385928	4.916526
H	3.649611	7.412532	6.317335
C	5.739827	7.713984	6.815091
H	6.628658	8.183018	6.386152
H	5.960414	6.654759	6.979533
H	5.535576	8.170747	7.784997
C	5.214207	13.310292	3.639686
C	5.266112	14.644449	3.217104
H	4.603711	15.379590	3.664993
C	6.164498	15.024830	2.225358
H	6.196995	16.061091	1.904600
C	7.017245	14.085170	1.647646
H	7.717251	14.383277	0.874497
C	6.960138	12.757109	2.073940
H	7.618897	12.017579	1.629691
C	6.066772	12.361298	3.063469
H	6.014983	11.332799	3.396836

Table S7: Cartesian coordinates for the B3LYP/6-311+G(d) optimized structure of *p*-NO₂.

O	1.166048	21.196603	15.718743
O	0.745955	22.073143	17.742104
O	-0.929236	14.642734	11.153427
O	-1.305192	13.020582	12.546736
N	0.035093	17.608869	16.631646
H	-0.023943	17.260462	17.595263
N	0.335111	18.881111	16.46075
N	0.256296	18.074786	19.220747
N	-1.010014	14.184627	12.28956
C	0.586531	19.688239	17.455541
C	0.837202	21.104004	17.016061
C	1.359049	22.536169	15.203483
H	2.154652	23.019607	15.774893
H	0.442044	23.107463	15.364272
C	1.705334	22.41372	13.734773
H	2.620314	21.834628	13.591154
H	1.861689	23.408365	13.308255
H	0.900452	21.928434	13.178203
C	0.619781	19.338711	18.89845
C	1.038561	20.236399	19.899201
H	1.313802	21.245913	19.637872
C	1.068325	19.813164	21.220579
H	1.388828	20.499196	21.997821
C	0.683122	18.512997	21.538397
H	0.690101	18.149043	22.559421
C	0.28674	17.684489	20.496361
H	-0.02025	16.659552	20.686564
C	-0.218099	16.791733	15.535919
C	-0.137006	17.269472	14.217475
H	0.130578	18.303287	14.045324
C	-0.396909	16.414884	13.159663
H	-0.339165	16.763933	12.13722
C	-0.736537	15.085403	13.412719
C	-0.820167	14.596529	14.715683
H	-1.0858	13.561451	14.883484
C	-0.561261	15.449917	15.774404
H	-0.624031	15.080382	16.792834

8 NMR Spectra

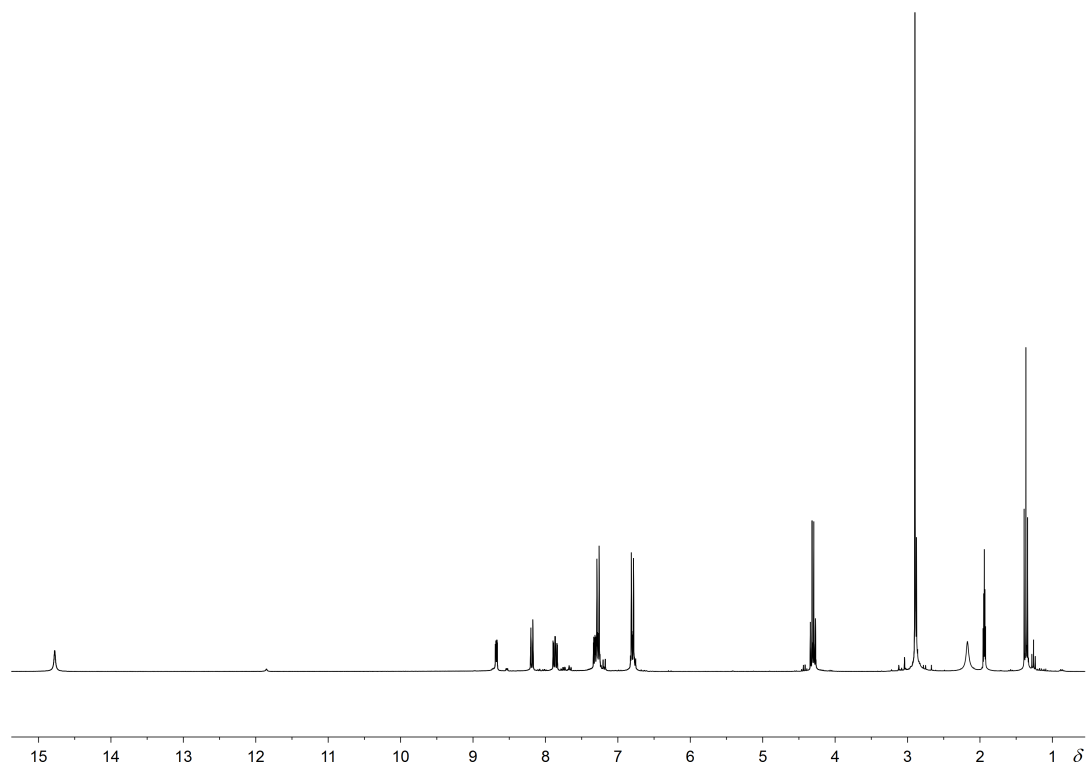


Figure S11: ¹H NMR spectrum of *p*-NMe₂ in CD₃CN at 294 K in the presence of the minor Z isomer.

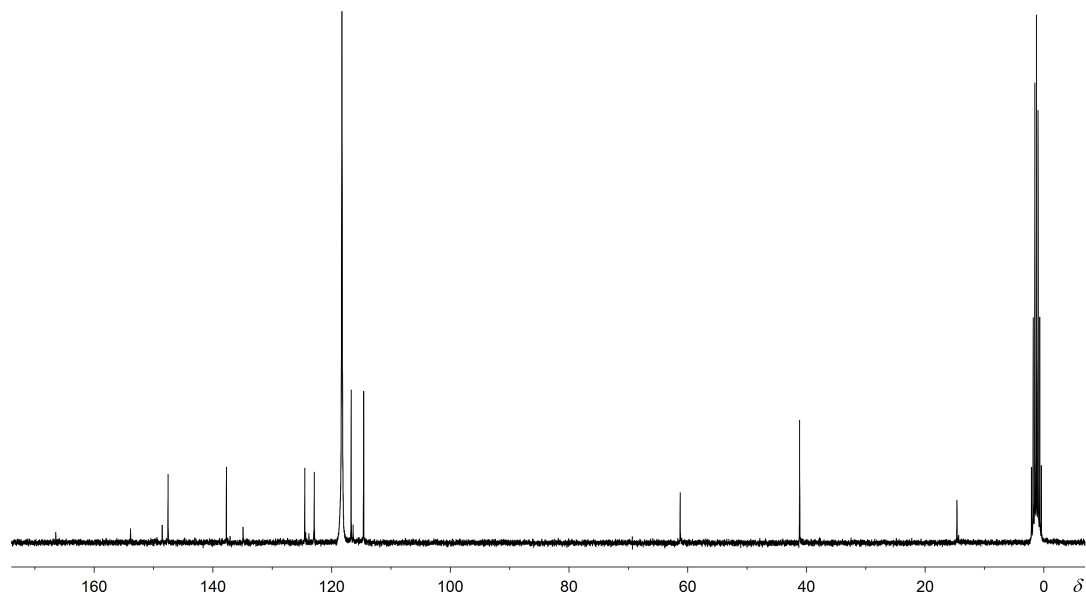


Figure S12: ¹³C NMR spectrum of *p*-NMe₂ in CD₃CN at 294 K in the presence of the minor Z isomer.

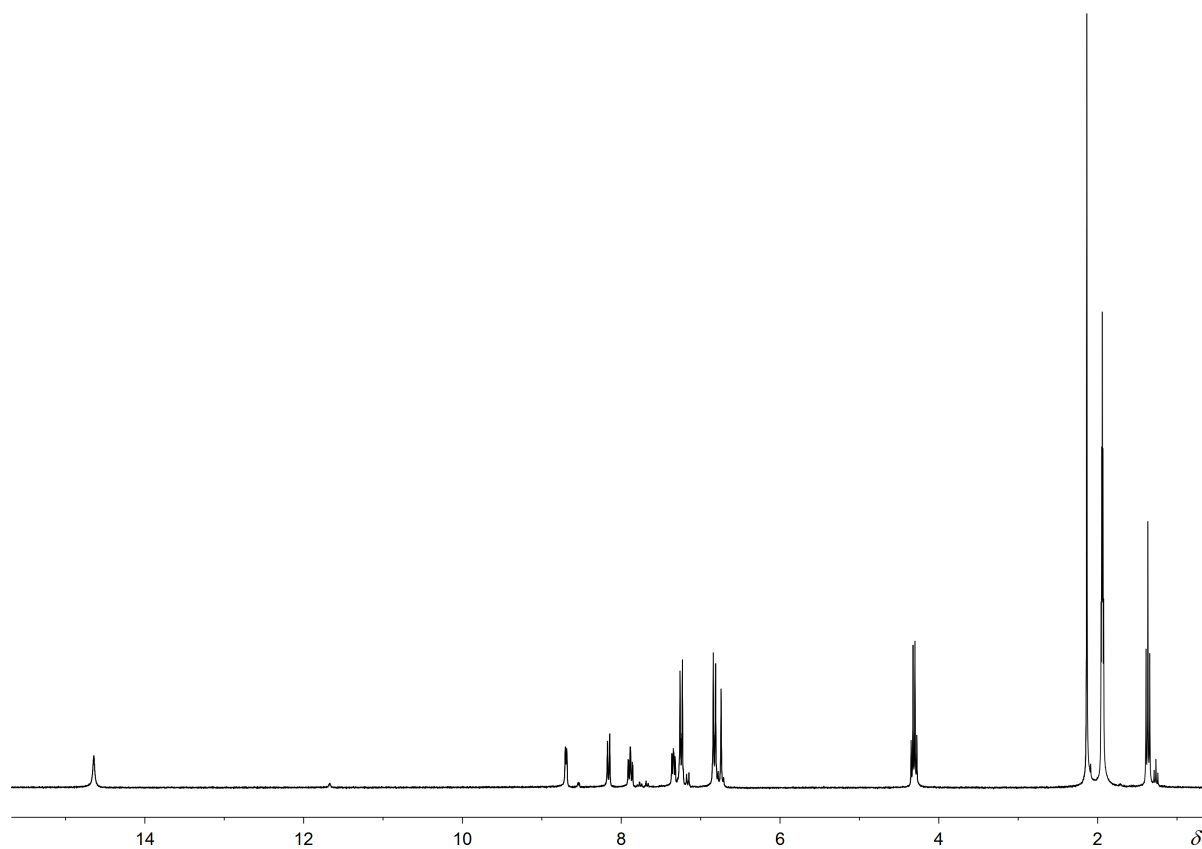


Figure S13: ¹H NMR spectrum of **p-OH** in CD₃CN at 294 K in the presence of the minor Z isomer.

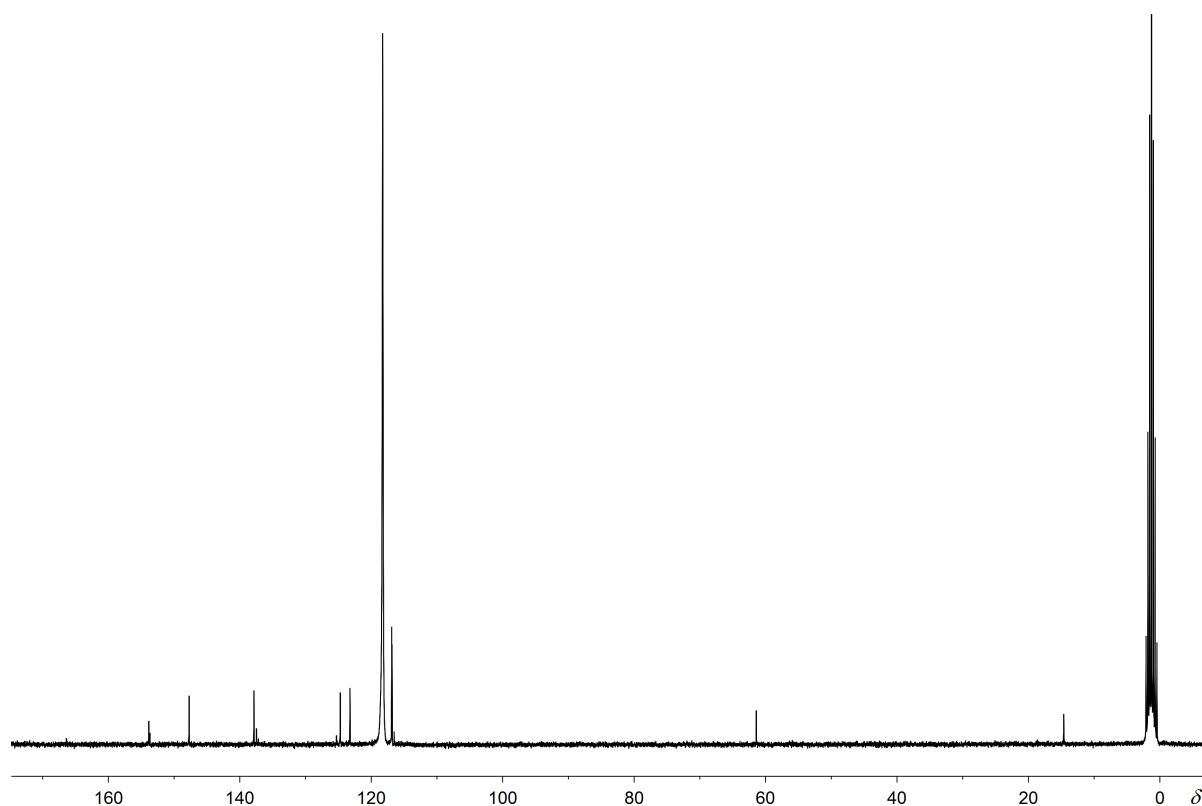


Figure S14: ¹³C NMR spectrum of **p-OH** in CD₃CN at 294 K in the presence of the minor Z isomer.

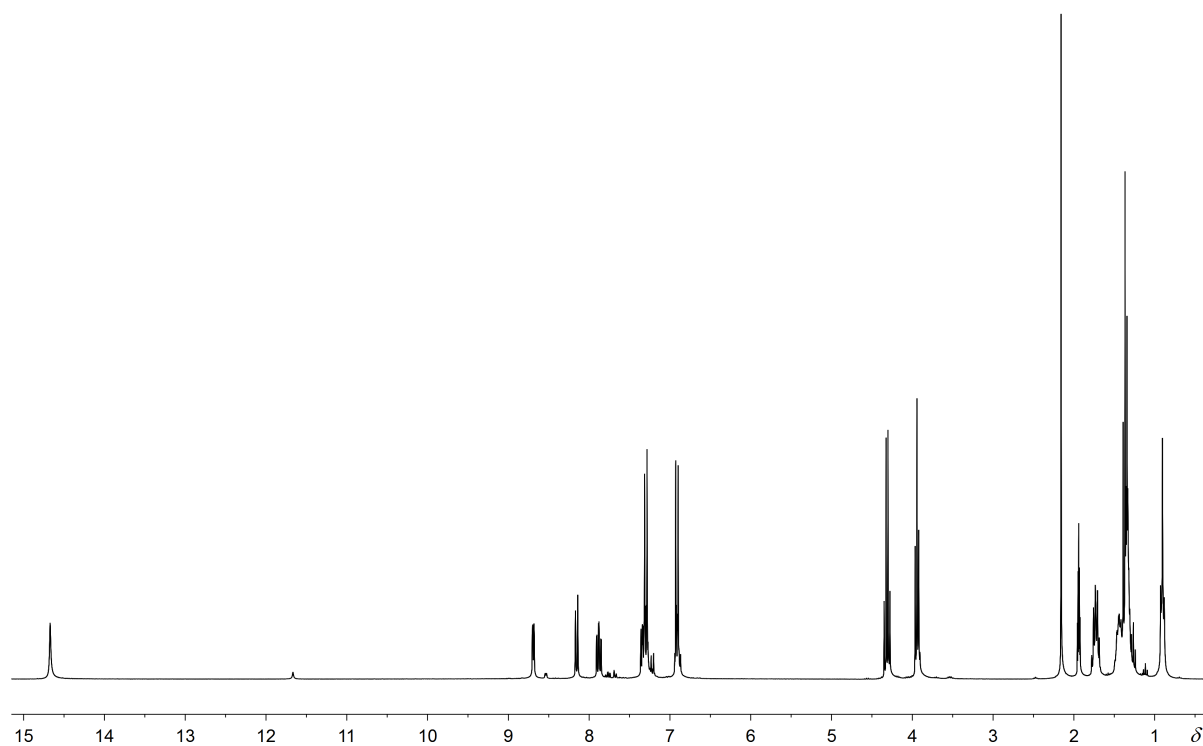


Figure S15: ¹H NMR spectrum of **p-OnHex** in CD₃CN at 294 K in the presence of the minor Z isomer.

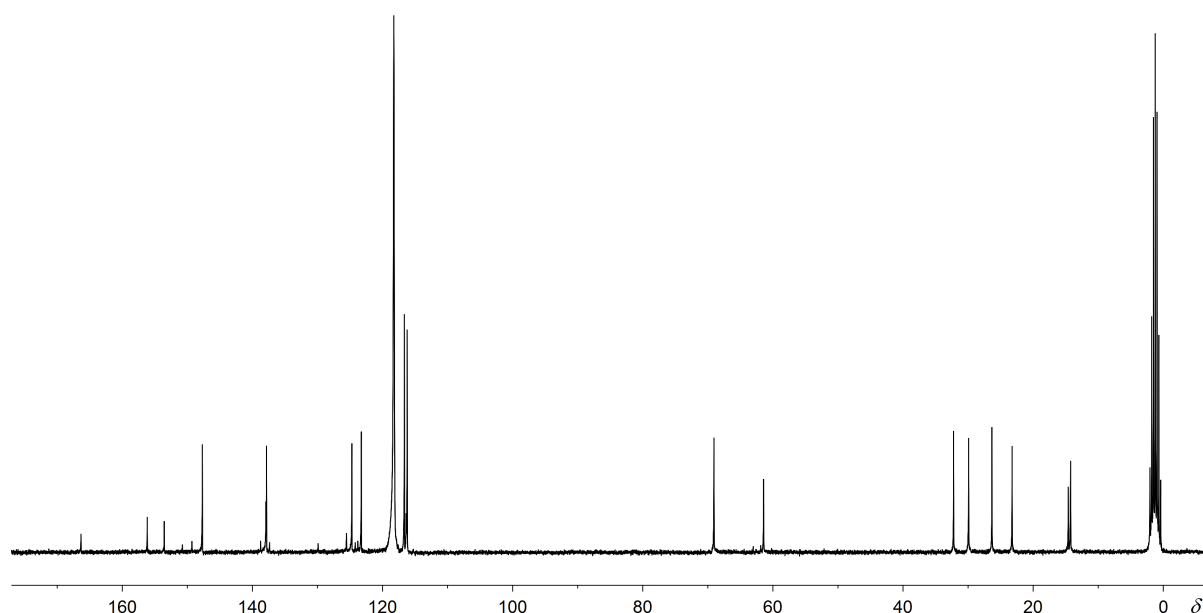


Figure S16: ¹³C NMR spectrum of **p-OnHex** in CD₃CN at 294 K in the presence of the minor Z isomer.

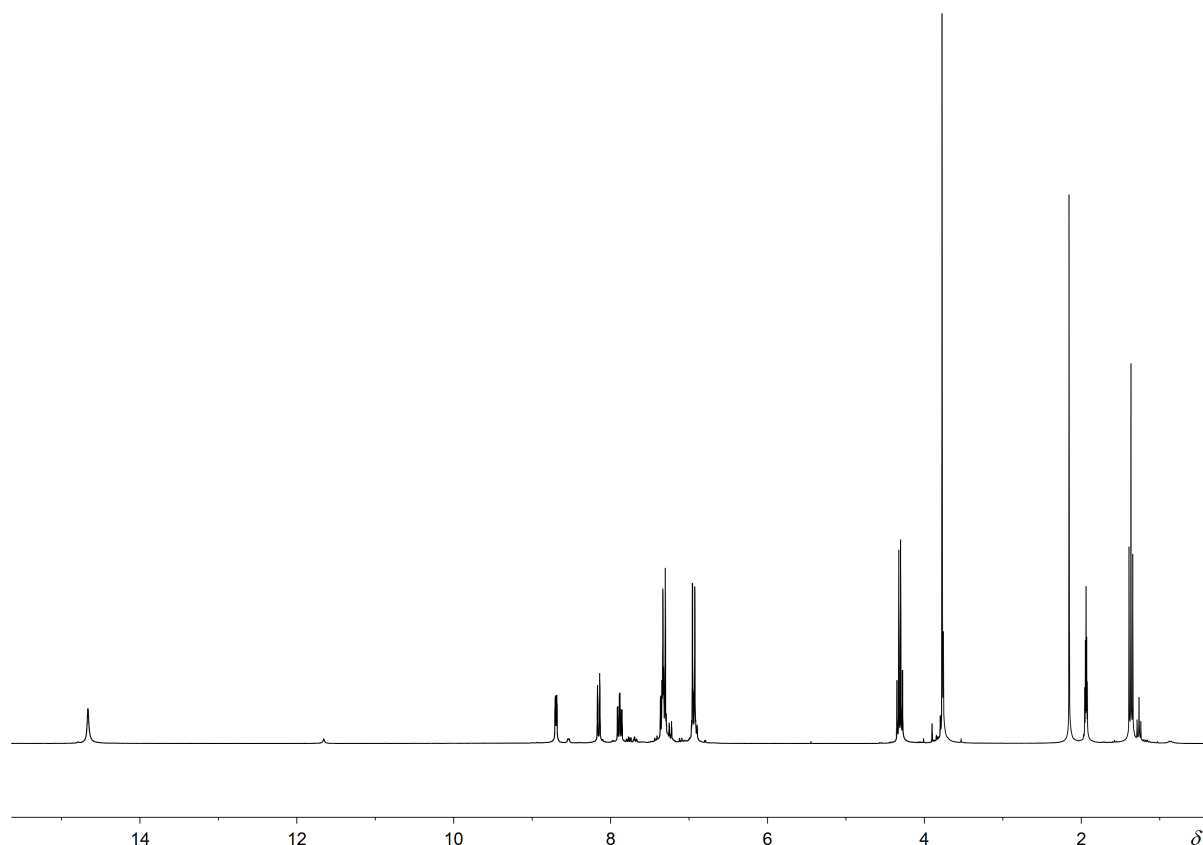


Figure S17: ¹H NMR spectrum of **p**-OMe in CD₃CN at 294 K in the presence of the minor Z isomer.

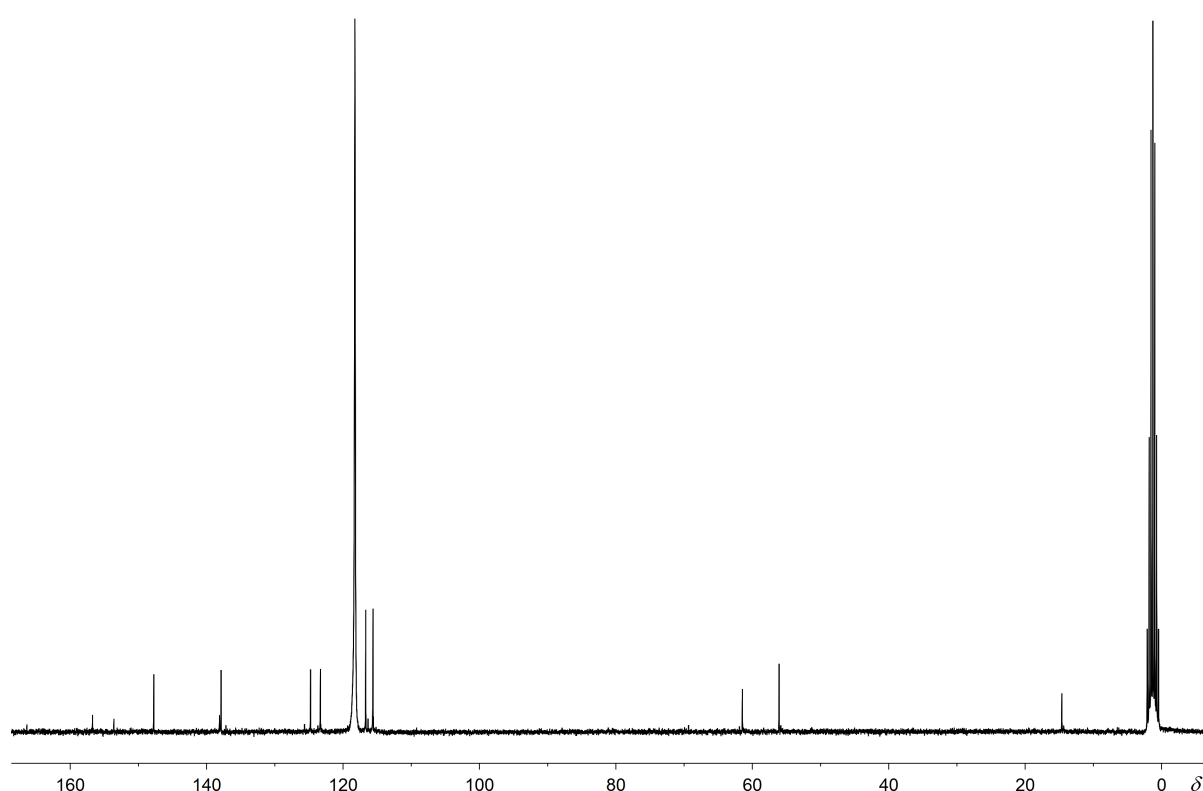


Figure S18: ¹³C NMR spectrum of **p**-OMe in CD₃CN at 294 K in the presence of the minor Z isomer.

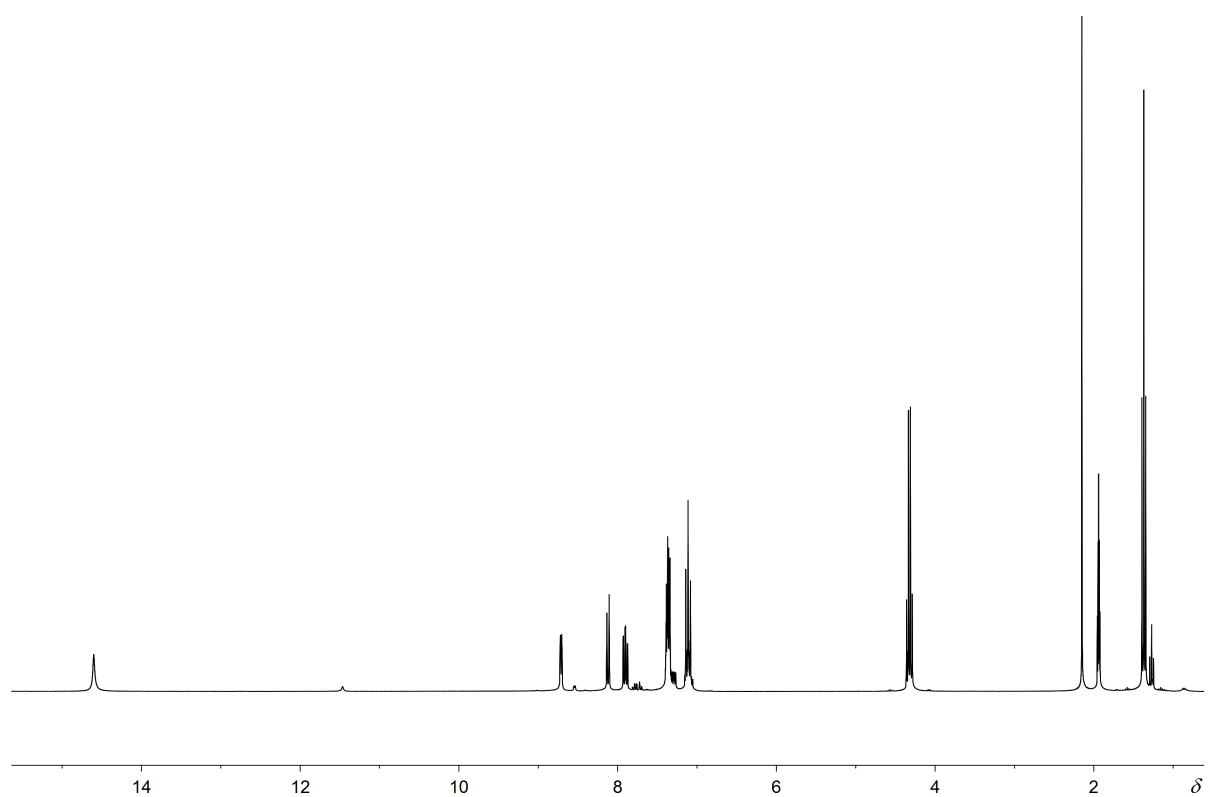


Figure S19: ¹H NMR spectrum of *p*-F in CD₃CN at 294 K in the presence of the minor Z isomer.

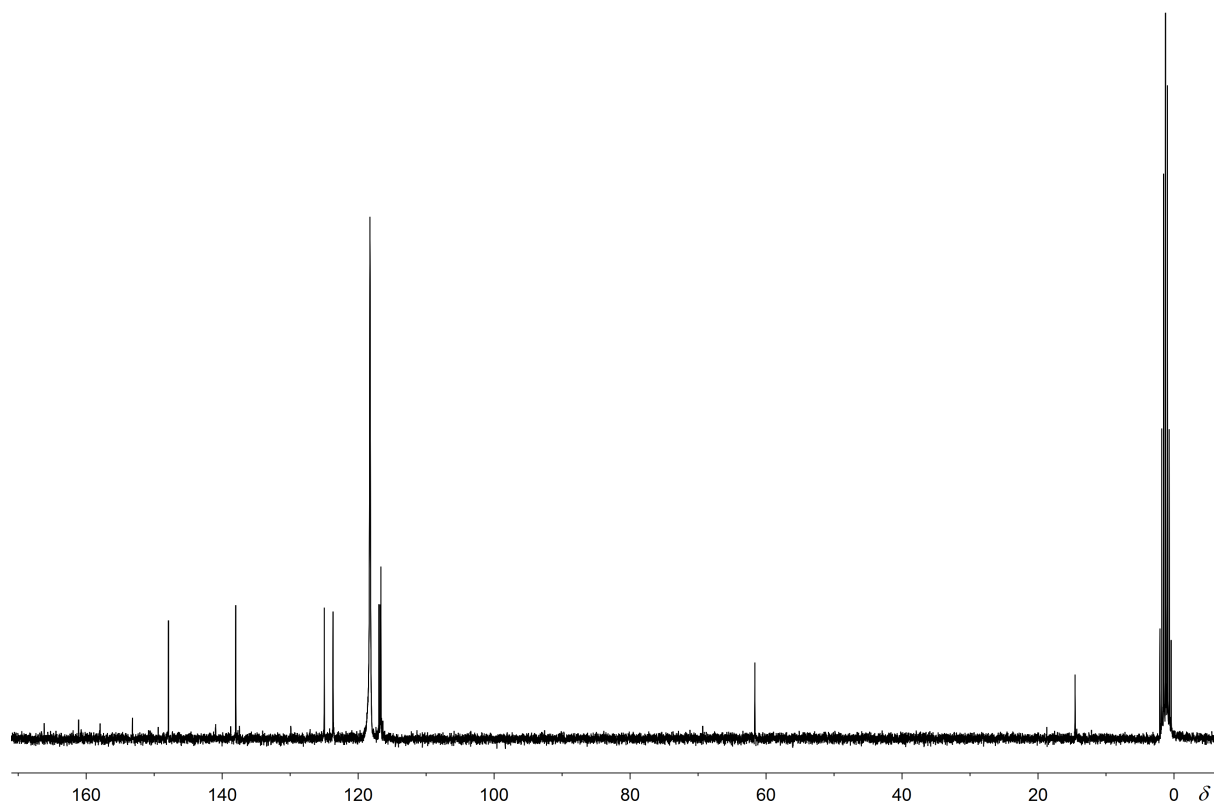


Figure S20: ¹³C NMR spectrum of *p*-F in CD₃CN at 294 K in the presence of the minor Z isomer.

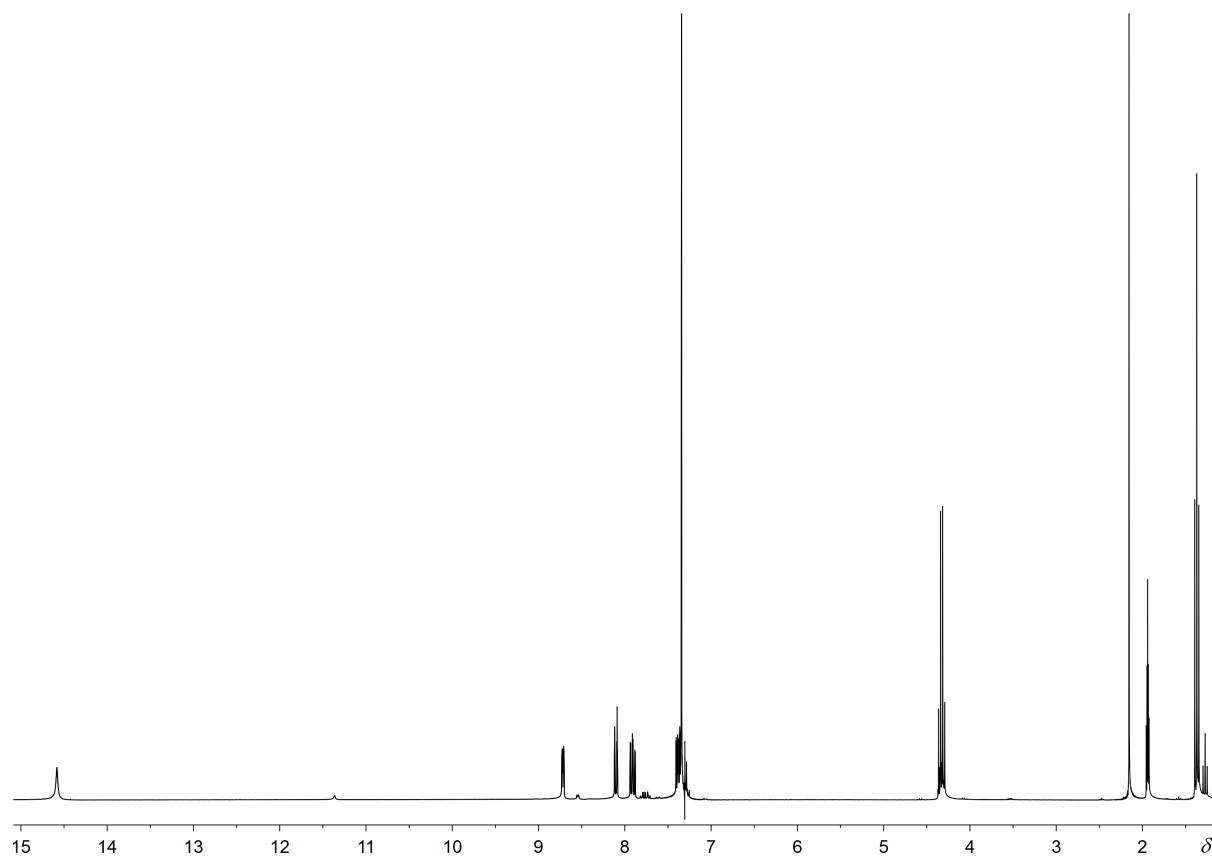


Figure S21: ¹H NMR spectrum of *p*-Cl in CD₃CN at 294 K in the presence of the minor Z isomer.

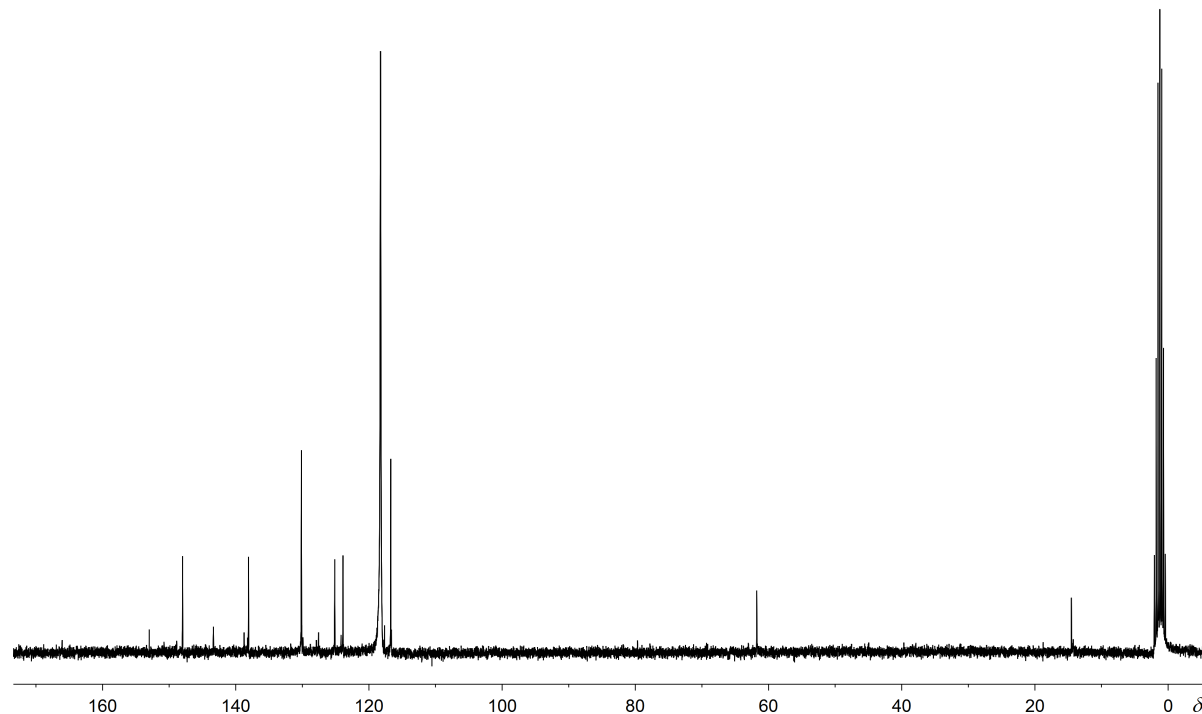


Figure S22: ¹³C NMR spectrum of *p*-Cl in CD₃CN at 294 K in the presence of the minor Z isomer.

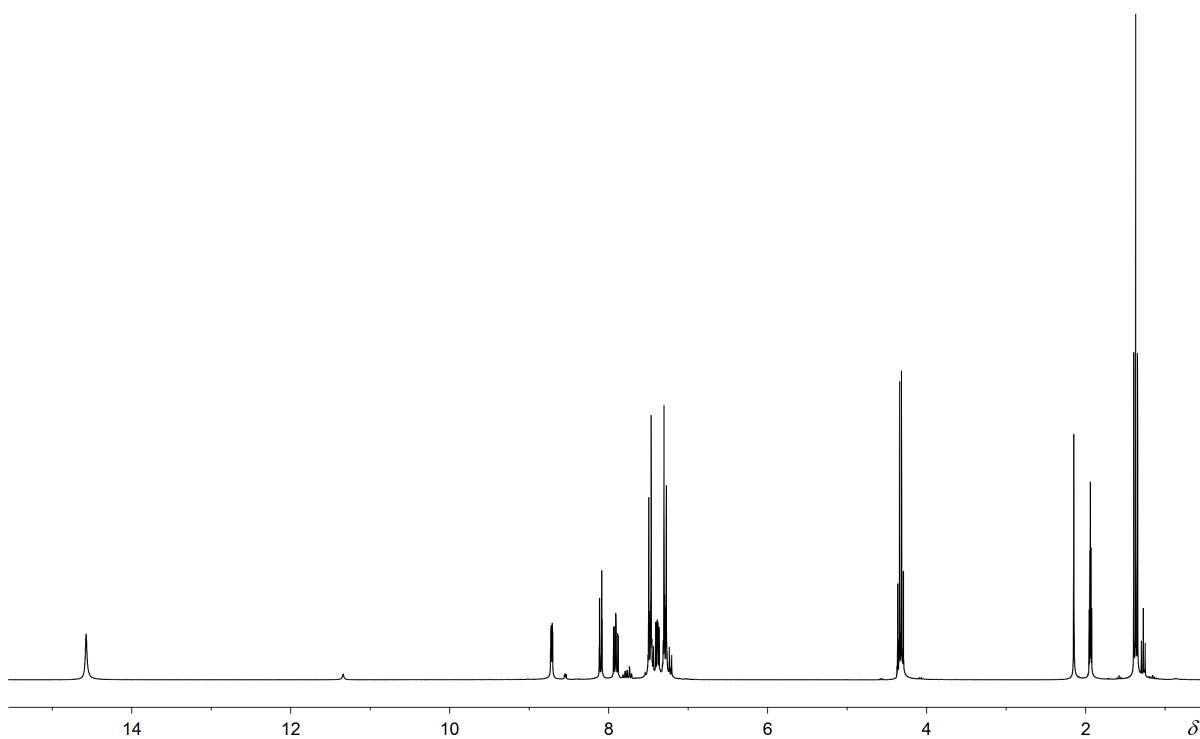


Figure S23: ${}^1\text{H}$ NMR spectrum of *p*-Br in CD_3CN at 294 K in the presence of the minor Z isomer.

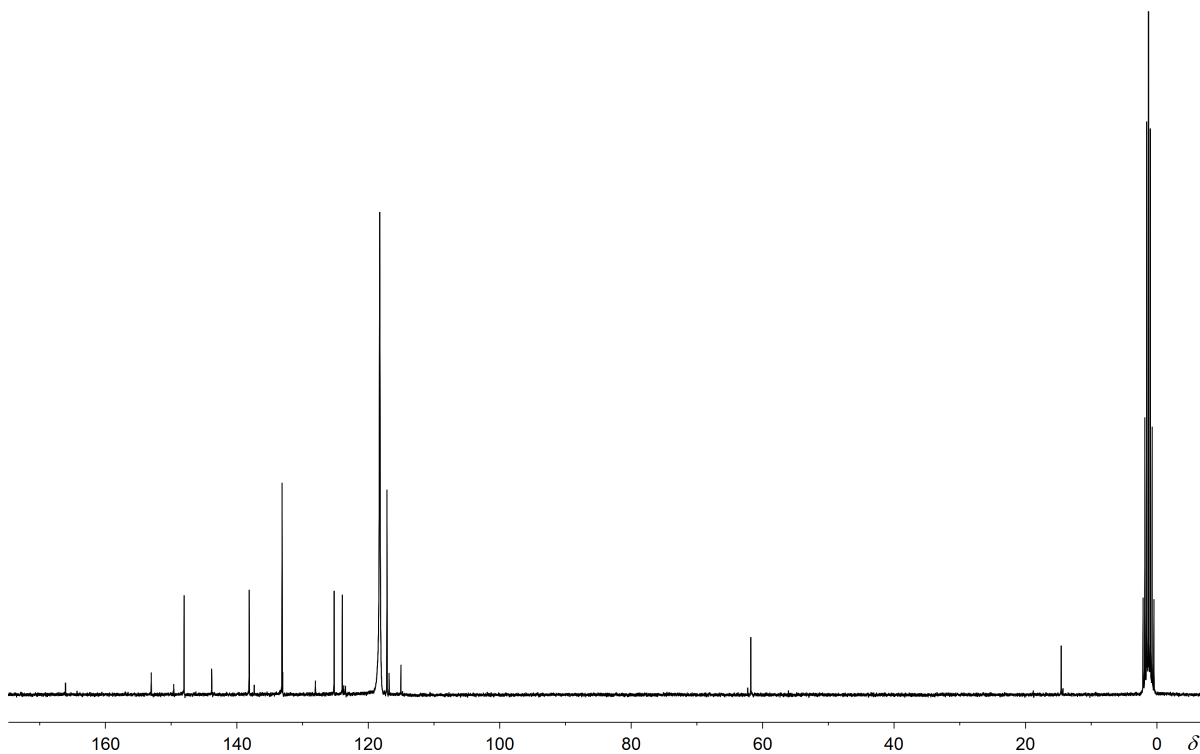


Figure S24: ${}^{13}\text{C}$ NMR spectrum of *p*-Br in CD_3CN at 294 K in the presence of the minor Z isomer.

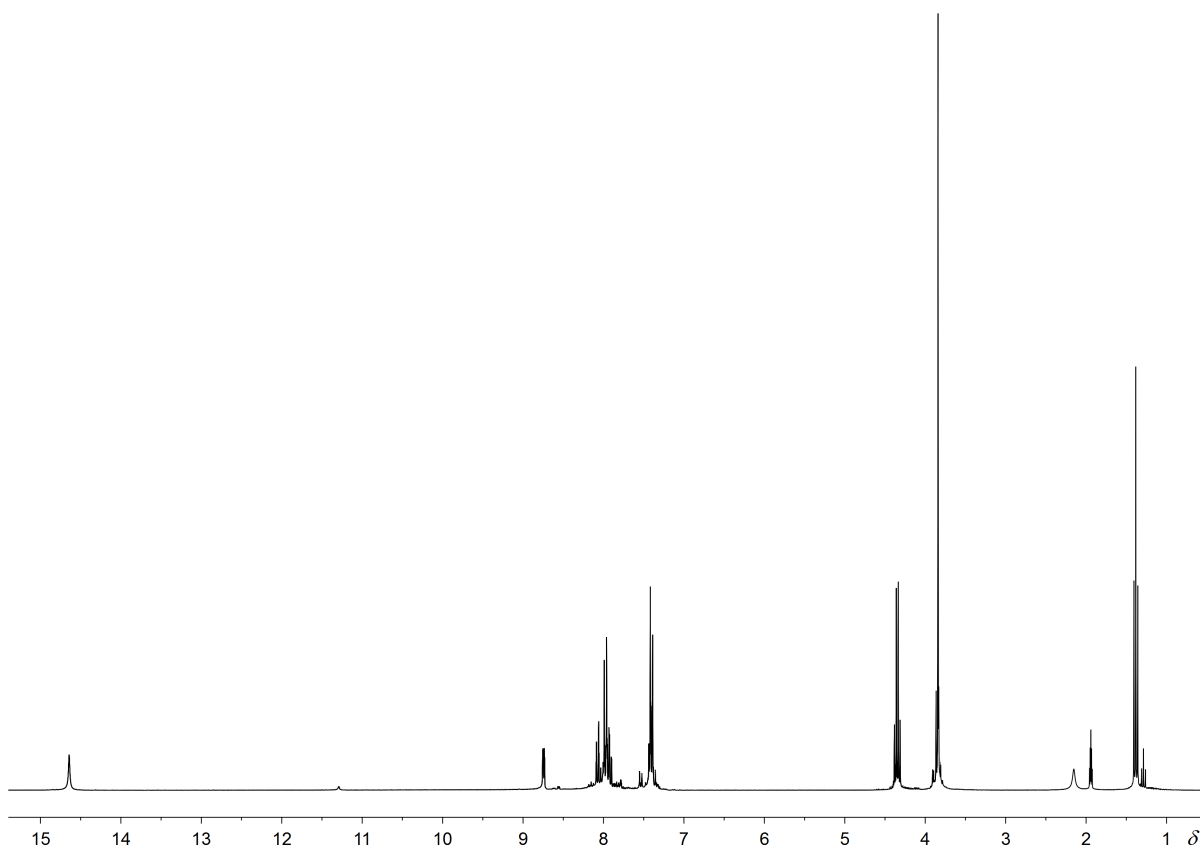


Figure S25: ¹H NMR spectrum of **p**-MC in CD₃CN at 294 K in the presence of the minor Z isomer.

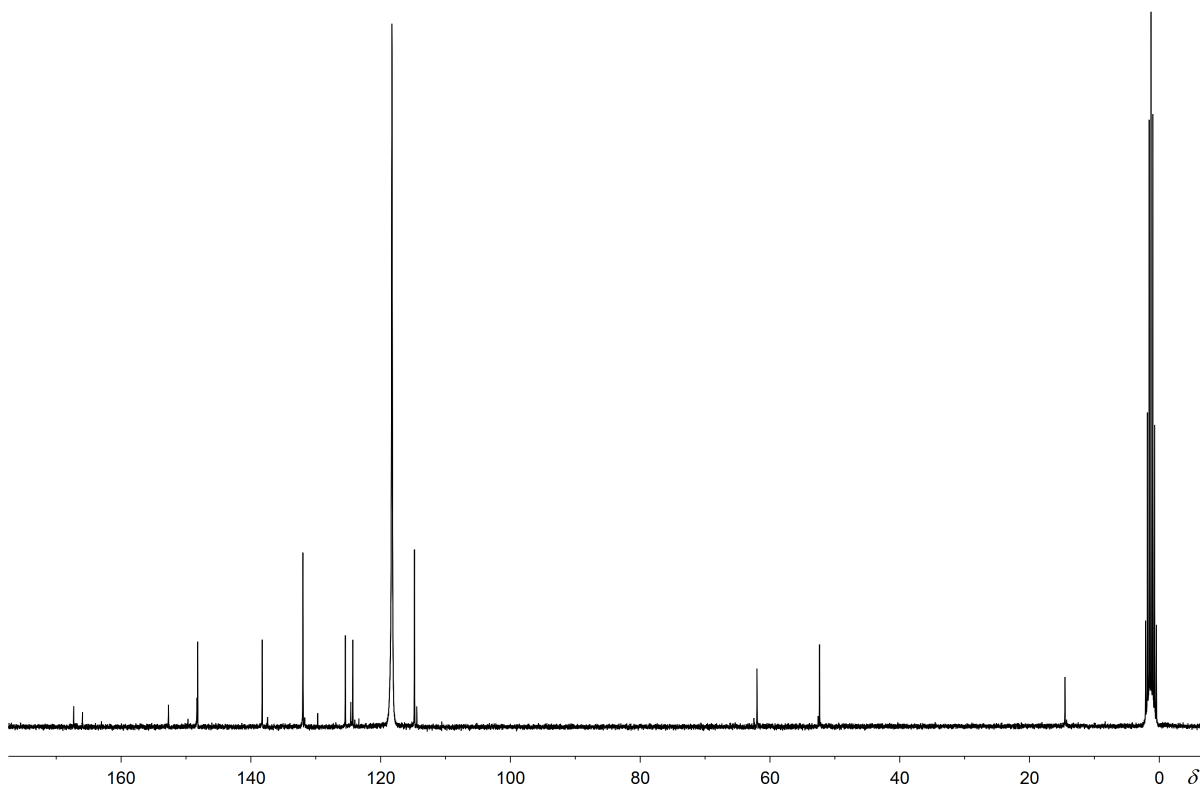


Figure S26: ¹³C NMR spectrum of **p**-MC in CD₃CN at 294 K in the presence of the minor Z isomer.

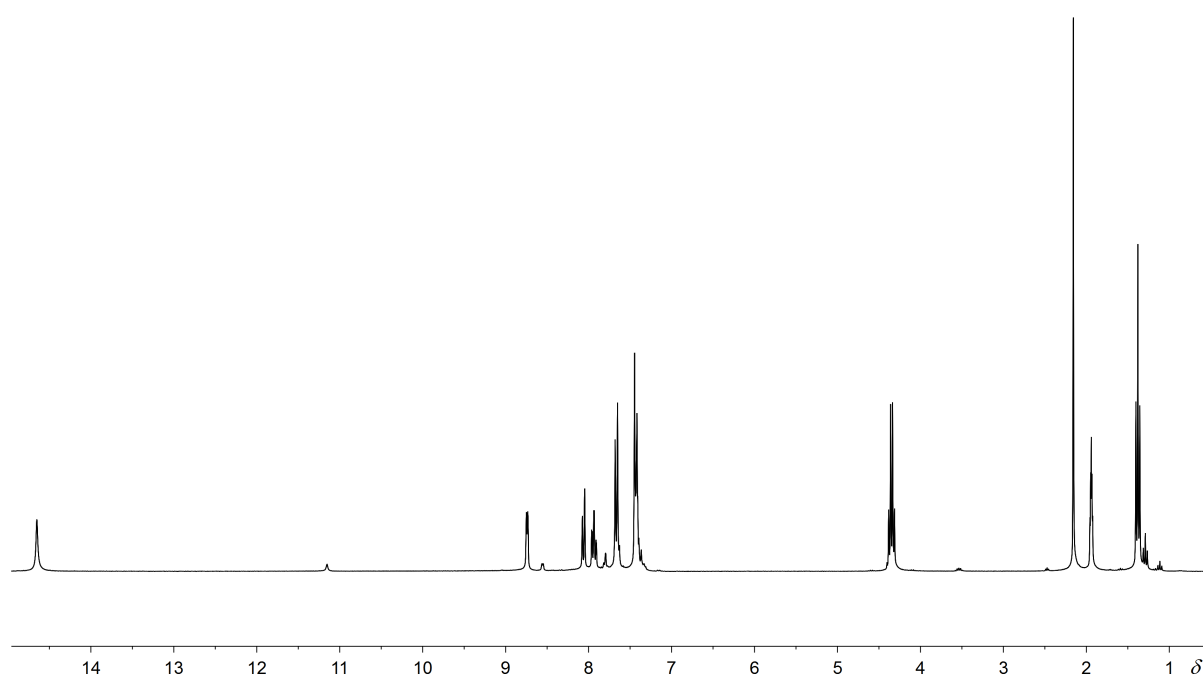


Figure S27: ¹H NMR spectrum of *p*-CN in CD₃CN at 294 K in the presence of the minor Z isomer.

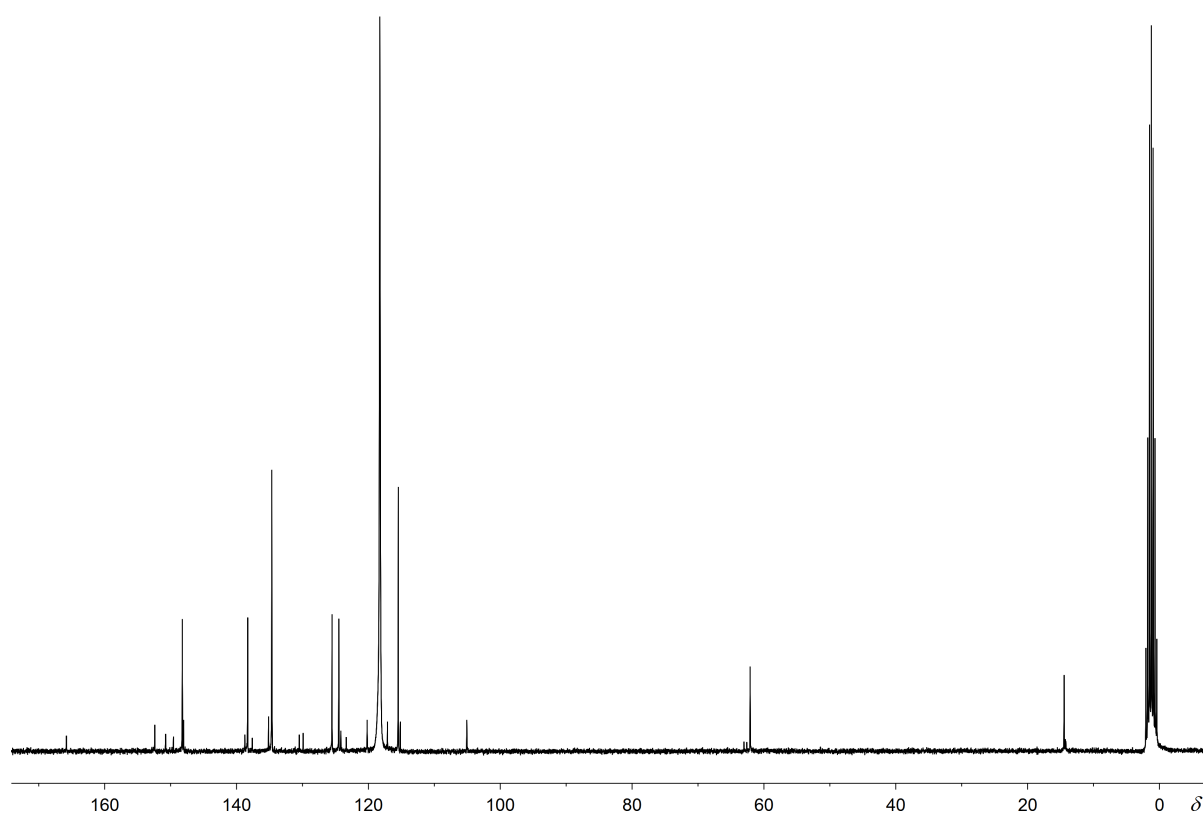


Figure S28: ¹³C NMR spectrum of *p*-CN in CD₃CN at 294 K in the presence of the minor Z isomer.

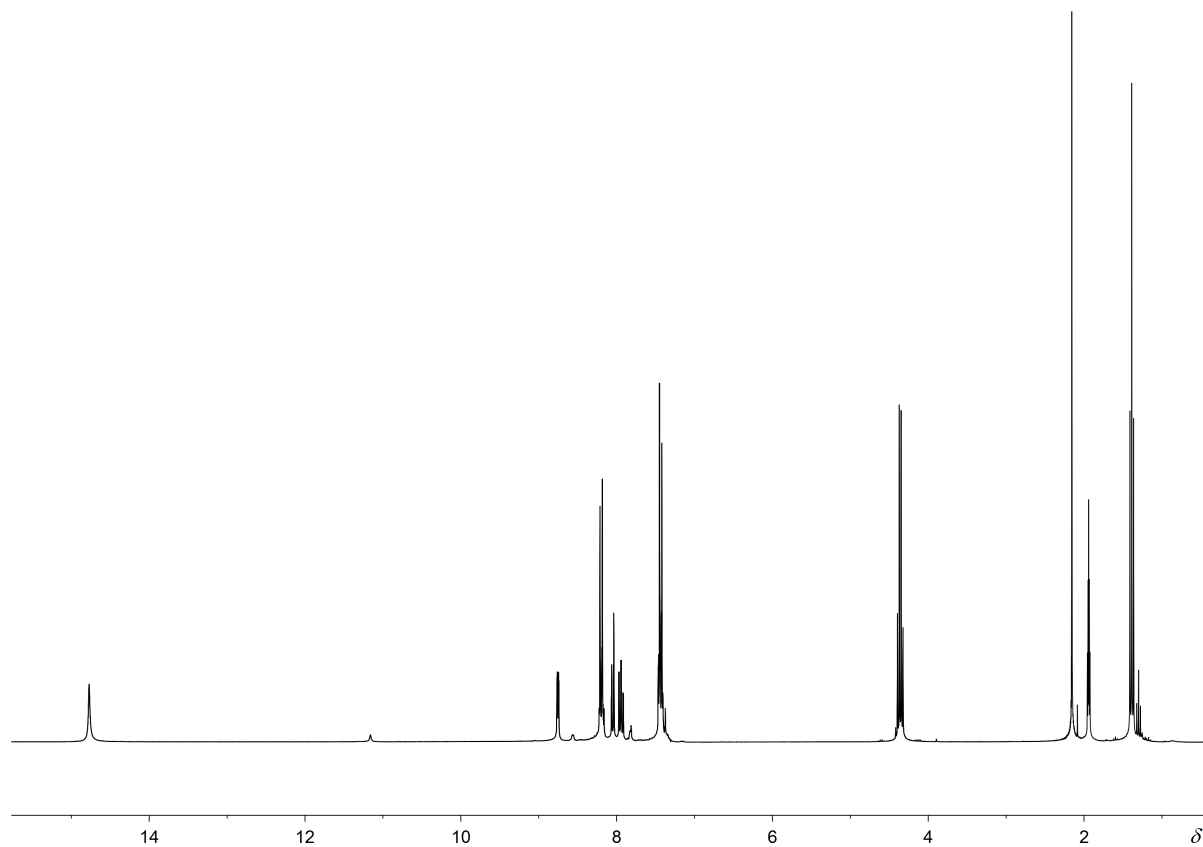


Figure S29: ¹H NMR spectrum of *p*-NO₂ in CD₃CN at 294 K in the presence of the minor Z isomer.

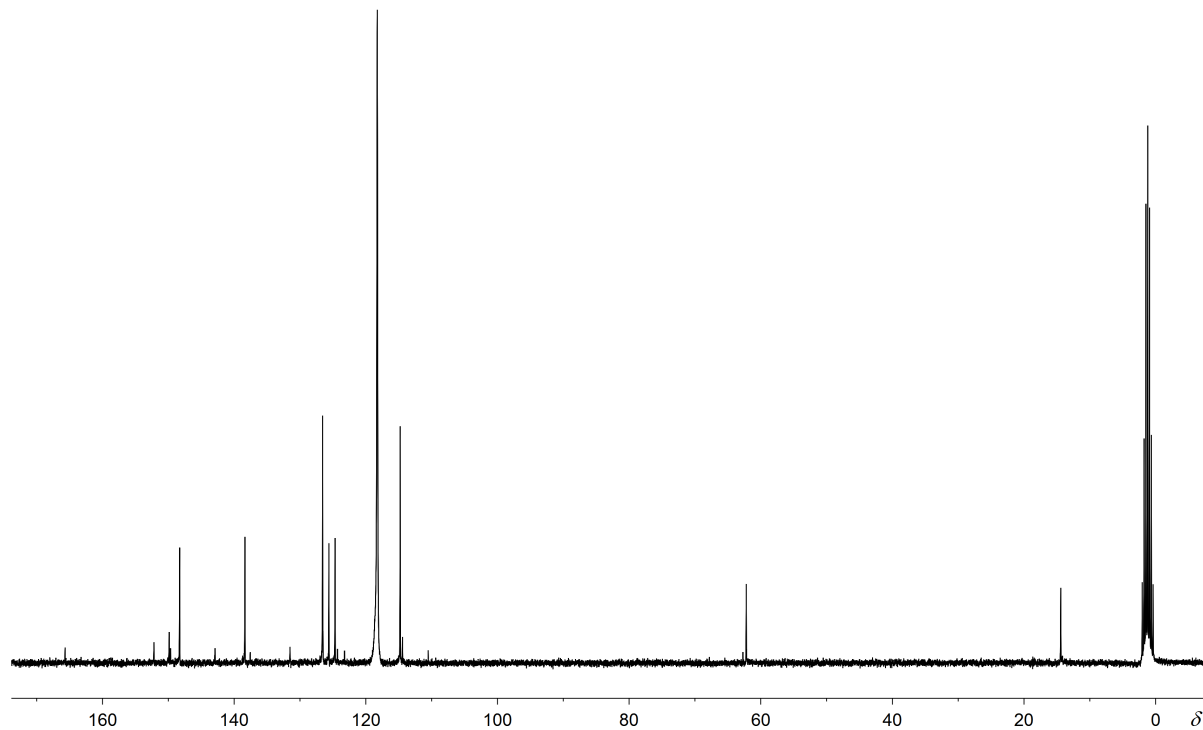


Figure S30: ¹³C NMR spectrum of *p*-NO₂ in CD₃CN at 294 K in the presence of the minor Z isomer.

References

- (S1) I. Kaljurand, A. Kütt, L. Sooväli, T. Rodima, V. Mäemets, I. Leito and I. A. Koppel, *J. Org. Chem.*, 2005, **70**, 1019–1028.
- (S2) L. Sooväli, I. Kaljurand, A. Kütt and I. Leito, *Anal. Chim. Acta*, 2006, **566**, 290–303.
- (S3) S. M. Landge, E. Tkatchouk, D. Benítez, D. A. Lanfranchi, M. Elhabiri, W. A. Goddard, III and I. Aprahamian, *J. Am. Chem. Soc.*, 2011, **133**, 9812–9823.
- (S4) Bruker Analytical X-ray Systems, Madison, WI, USA, *COSMO V1.58, Software for the CCD Detector Systems for Determining Data Collection Parameters*, 2008.
- (S5) Bruker Analytical X-ray Systems, Madison, WI, USA, *APEX2 V2008.5-0 Software for the CCD Detector System*, 2008.
- (S6) Bruker Analytical X-ray Systems, Madison, WI, USA, *SAINT V 7.34 Software for the Integration of CCD Detector System*, 2008.
- (S7) R. H. Blessing, *Acta Cryst. A*, 1995, **51**, 33–38.
- (S8) G. M. Sheldrick, *Acta Cryst. A*, 2008, **64**, 112–122.
- (S9) (a) C. Lee, W. Yang and R. G. Parr, *Phys. Rev. B*, 1988, **37**, 785–789; (b) A. D. Becke, *J. Chem. Phys.*, 1993, **98**, 5648–5652; (c) P. J. Stephens, F. J. Devlin, C. F. Chabalowski and M. J. Frisch, *J. Phys. Chem.*, 1994, **98**, 11623–11627.
- (S10) M. J. Frisch, G. W. Trucks, H. B. Schlegel, G. E. Scuseria, M. A. Robb, J. R. Cheeseman, G. Scalmani, V. Barone, B. Mennucci, G. A. Petersson, H. Nakatsuji, M. Caricato, X. Li, H. P. Hratchian, A. F. Izmaylov, J. Bloino, G. Zheng, J. L. Sonnenberg, M. Hada, M. Ehara, K. Toyota, R. Fukuda, J. Hasegawa, M. Ishida, T. Nakajima, Y. Honda, O. Kitao, H. Nakai, T. Vreven, J. A. Montgomery, Jr., J. E. Peralta, F. Ogliaro, M. Bearpark, J. J. Heyd, E. Brothers, K. N. Kudin, V. N. Staroverov, R. Kobayashi, J. Normand, K. Raghavachari, A. Rendell, J. C. Burant, S. S. Iyengar, J. Tomasi, M. Cossi, N. Rega, J. M. Millam, M. Klene, J. E. Knox, J. B. Cross, V. Bakken, C. Adamo, J. Jaramillo,

R. Gomperts, R. E. Stratmann, O. Yazyev, A. J. Austin, R. Cammi, C. Pomelli, J. W. Ochterski, R. L. Martin, K. Morokuma, V. G. Zakrzewski, G. A. Voth, P. Salvador, J. J. Dannenberg, S. Dapprich, A. D. Daniels, Ö. Farkas, J. B. Foresman, J. V. Ortiz, J. Cioslowski, and D. J. Fox, *Gaussian 09 Revision A.1*, Gaussian Inc. Wallingford CT 2009.